Impact of water and tillage erosion on soil organic carbon stability

Auteur : Verjans, Pierre
Promoteur(s) : Meersmans, Jeroen; Colinet, Gilles
Faculté : Gembloux Agro-Bio Tech (GxABT)
Diplôme : Master en bioingénieur : sciences et technologies de l'environnement, à finalité spécialisée
Année académique : 2022-2023
URI/URL : http://hdl.handle.net/2268.2/18292

LIÈGE université
Gembloux
Agro-Bio Tech

Impact of water and tillage erosion on soil organic carbon stability

Pierre Verjans

MASTER THESIS PRESENTED FOR THE OBTAINING OF A DEGREE IN BIOENGINEERING IN ENVIRONMENTAL SCIENCES AND TECHNOLOGIES

ACADEMIC YEAR 2022 - 2023

PROMOTERS: Pr. Gilles Colinet, Pr. Jeroen Meersmans

LIÈGE université
Gembloux
Agro-Bio Tech

Impact of water and tillage erosion on soil organic carbon stability

Pierre Verjans

MASTER THESIS PRESENTED FOR THE OBTAINING OF A DEGREE IN BIOENGINEERING IN ENVIRONMENTAL SCIENCES AND TECHNOLOGIES

ACADEMIC YEAR 2022 - 2023

PROMOTERS: Pr. Gilles Colinet, Pr. Jeroen Meersmans

Remerciements

Aux derniers jours de la rédaction de ce TFE, qui marque la fin de mon parcours d'étudiant, j'aimerais remercier les nombreuses personnes qui ont rendu la réalisation de ce travail possible et enrichissante.

Tout d'abord, je remercie mes promoteurs Jeroen Meersmans et Gilles Colinet pour m'avoir, dans un premier temps, initié à l'étude des sols, et pour m'avoir permis ensuite de réaliser mon TFE sur le sujet passionnant du carbone des sols. Merci également pour l'énergie investie dans la transmission de connaissances qui ont fait de ce travail un formidable apprentissage. Je remercie Nicolas Kovacs pour l'aide précieuse accordée sans compter. D'une manière plus générale, je remercie les membres du jury pour l'attention qu'ils portent à ce travail.

Je remercie Emmanuel Vranckx pour l'accès laissé à sa parcelle ainsi que pour la confiance et l'autonomie accordées. Je remercie également Pierre Baert pour la transmission rapide des données établies par son travail.

Je remercie Stephane Becquevort et Gilles Swerts pour le matériel de terrain et l'accès au laboratoire du bâtiment Topo.

Je remercie le personnel du GP, en particulier Emilie Marit et Pauline Biron pour leur aide, leur patience à toute épreuve et leur bonne humeur.

Je remercie Claire Spiroux, Nahama Brutout et Guillaume Bernard pour le courage qui les a fait se lever tôt un matin pour affronter la pluie.

De plus, j'aimerais remercier toutes les personnes qui m'ont accompagné de près lors de ces 5 années d'études. Même si j'en oublie certains, j'imagine que vous n'aurez pas besoin de ces quelques lignes pour connaître ma gratitude, qu'il est difficile de faire transparaître par écrit.

Je remercie ma famille pour son soutien, particulièrement ma mère, qui m'a transmis le plaisir d'apprendre et qui a fait de mon parcours scolaire une réussite dont je mesure la chance.

Je remercie mes cokoteurs pour cette année de cohabitation à peine agitée, la team STE pour cette belle année de ma1, les Marseillais pour les vacances juste bien, le CB pour leurs idées farfelues, Peyresq pour les souvenirs que je m'y suis fait, les Epioux pour ces deux week-end hors du temps, le comité AG pour votre sérieux et tous les beaux projets qu'on a réalisés, et les OF7 pour votre non-sérieux et tous les délires qu'on a réalisés. Je remercie tous ceux avec qui j'ai eu la chance de participer à la vie AGéenne. J'ai parfois le sentiment d'avoir appris plus de choses à vos côtés que sur les bancs des auditoires.

Abstract

Soils represent one of the largest carbon (C) pools on Earth. Therefore, they have a major potential to regulate atmospheric CO_2 concentrations. Moreover, high soil C contents in croplands offer numerous advantages, leading to the interest in establishing soil C sequestration policies. Therefore, having a good understanding of soil C dynamics is crucial. This study quantifies the effects of water and tillage erosion, which are part of the principal soil degradation processes, on soil carbon stability. Six plots representing different intensities of both water and tillage erosion in the Belgian loess belt have been studied. Measurements of soil organic carbon (SOC) stocks showed the redistribution of C from eroded plots to plots undergoing sediment deposition, where important quantities of C are buried to lower horizons. Measurements of soil respiration carried out at 11 different days from March to July revealed that soil C mineralisation rates at eroded locations are two times higher than at deposition locations. Deposition locations present lower mineralisation rates than non-eroded locations. Deposition locations are also characterised by low temperature sensitivities of soil C mineralisation rates. The observed higher stability of the deposition locations can be explained by higher subsoils SOC stocks, higher concentrations of biochemically recalcitrant organic C, and higher proportions of organic C chemically bounded to soil particles. These observations highlight the effects of erosion processes on SOC distribution and SOC stability, and thus, on soil C dynamics. Conclusions give a first quantification of the impact of erosion on C sequestration by croplands and call for a larger-scale study including other erosion-induced processes.

Key words: soil organic carbon, erosion, carbon stability, soil respiration, Belgian loess belt

Résumé

Les sols représentent l'un des plus grands réservoirs de carbone (C) sur Terre. C'est pourquoi ils ont un potentiel majeur quant à la régulation de la concentration en CO_2 atmosphérique. De plus, de hautes teneurs en C dans les sols présentent de nombreux avantages, poussant à la mise en place de politiques de séquestration de C par les sols. Dès lors, avoir une bonne compréhension de la dynamiques du C des sols est crucial. Cette étude quantifie les effets de l'érosion hydrique et de labour, qui fait partie des principales formes de dégradation des sols, sur la stabilité du C des sols . Six parcelles expérimentales, représentant différentes intensités d'érosion hydrique et de labour en Hesbaye, ont été étudiées. Les mesures de stock de carbone organique du sol (COS) ont montré une redistribution du C des sites érodés vers les sites de dépôt, où d'importantes quantités de C sont enterrées vers les horizons inférieurs. Les mesures de respiration du sol, menées lors de 11 jours entre mars et juillet, ont révélé que les taux de minéralisation du C étaient deux fois plus grands aux parcelles érodées qu'aux parcelles de dépôt. Les parcelles de dépôts présentent des taux de minéralisation plus bas que ceux de la parcelle non-affectée par l'érosion. Les parcelles de dépôt sont également caractérisées par de faibles sensibilités des taux de minéralisation aux hausses de températures. La stabilité observée aux parcelles de dépôt peut être expliquée par de plus grands stocks de COS en profondeur, de plus grandes concentrations en C biochimiquement récalcitrant et de plus grandes proportion de C chimiquement lié aux particules du sol. Ces observations témoignent des effets des processus d'érosion sur la distribution du COS et sa stabilité et, par extension, sur la dynamique du C des sols. Les conclusions obtenues permettent une première quantification de l'impact de l'érosion sur la séquestration de C par les terres agricoles et appellent à une étude à plus grande échelle, incluant d'autres processus provoqués par l'érosion.

Mots clés: carbone organique des sols, érosion, stabilité du carbone, respiration du sol, Hesbaye

Table of contents

List of Figures

List of Tables

Acronyms

CO_2 : carbon dioxide
F_s : soil CO_2 flux
HF : heavy fraction
LF : light fraction
RUSLE : revised universal soil loss equation
RMSE : root mean squared error
SOC : soil organic carbon
WB : Walkley and Black
WC : water content

1 Introduction

1.1 Context

The worldwide stock of soil organic carbon (SOC) within the 1st meter of soil is estimated between 1500 Pg (10^{15}g) and 2400 Pg of carbon (C) (Smith et al., 2020). Even with the smallest estimation, soils represent a carbon stock twice as large as the atmosphere and three times as large as the world vegetation. Thus, they represent a critical carbon reservoir, capable of acting either like a C sink or a source to the atmosphere (Martin et al., 2011). An illustration of this major potential is the fact that conversion of landform from their native states to agricultural land, diminishing the SOC content of those soils, was responsible for around a third of $CO2$ emissions between 1870 and 1980 (Harden et al., 1999).

Sequestrating C in soils does not only address environmental problematics, it also has a primary role in agrosystems (Balesdent, 1996). Organic matter greatly contributes at soil structuration, facilitating root penetration, water infiltration and water retention and increasing soil resistance to compaction and erosion. It also strongly contributes to nutrient retention in soils and nutrient availability for plants with multiple mechanisms such as sorption and desorption, dissolution of organo-metallic complexes in soil solution and mineralization (Gerke, 2022). Soil organic matter also represents the main energy source for soil macro- and microfauna which are drivers of nutrient cycle and plant productivity (Beule et al., 2022).

Finally, SOC also responds to sanitary issues, notably water pollution by pesticides or nitrates, by retaining contaminants during their way to surface water or groundwater (Poissant et al., 2008). In Belgium, aquifers provide drinking water and require therefore a good quality control to limit frequent contaminations in components such as bentazone (Hakoun et al., 2017).

Nevertheless, SOC stocks in Belgian croplands have decreased in the second half of the 20th century (van Wesemael et al., 1960 ; Meersmans et al., 2011). Current agricultural practices expose soils to more intense soil degradation processes such as erosion or acidification, having a direct impact on SOC stocks (Frank et al., 2015). Environmental factors also play a role on those stocks. Concerns are raised that increasing temperatures will set up a feedback loop by inhibiting soil carbon sequestration.

As shown previously, the benefits of soil carbon sequestration can be found in multiple areas. Soil carbon policies would therefore cause, in addition to CO_2 emissions reduction, many other co-benefits. This makes them more inclusive solutions in comparison with other climate mitigation policies (Glenk and Colombo, 2011). However, the factors facilitating or inhibiting soil carbon sequestration are not fully understood, and this work fall within the numerous studies of the last decades trying to establish a more complete comprehension of soil carbon dynamics. In particular, this study will focus on **the impact of water and tillage erosion on soil carbon stability** to determine whether those processes play an inhibitor or facilitator role in carbon sequestration. As mentioned in the following sections, those factors could have significant roles on soil carbon stability which have not been completely understood yet.

1.2 Soil carbon dynamics

Soil carbon sequestration is the process of removing carbon from the atmosphere and storing it in the soil. Reducing atmospheric carbon mainly occurs by photosynthesis. The net annual flux of C between atmosphere and land represents as much as 123 Pg (Lal, 2013). This flux is called "gross primary productivity" (GPP). Part of it is released to the atmosphere by leaf, stem and root respiration, resulting in a "net primary productivity" (NPP) of 60 Pg/year. This quantity is the amount of C captured and not directly released back to the atmosphere by plants.

After the harvest, the remaining biomass and organic amendments represent a carbon input for soils (figure 1). It arrives in the soil in a relatively big and fresh form, called particular organic matter (POM), and is then changed into more stable soil organic matter (SOM) after microbial decomposition (Stockmann, 2012). Soil microbes achieve depolymerization and exudation, releasing processed C in soil solution, where it can form mineral associations with soil particles (Dynarski et al., 2020). However, microbial activity goes along with heterotrophic respiration, sending part of the carbon input back to the atmosphere. It is important to consider the soil organic cycle as a dynamic cycle: SOM can be sorbed and desorbed from soil particles, be buried to lower soil profiles, be re-decomposed, etc.

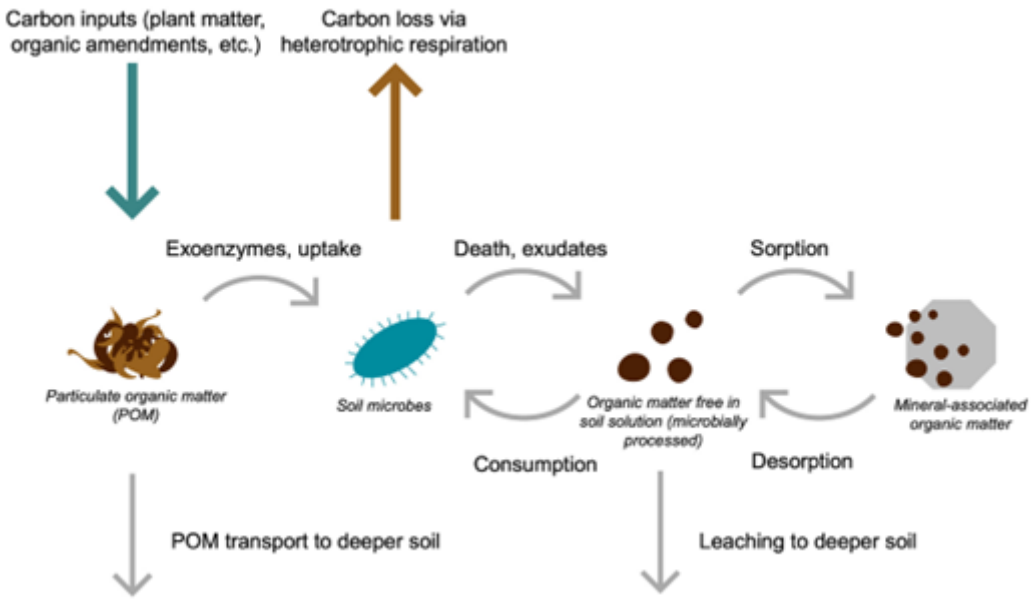

Figure 1: Topsoil carbon dynamics (Dynarski et al., 2020). Carbon inputs are in form of particulate organic matter (POM). After degradation by micro-organisms, soil organic matter (SOM) can be found in soil solution or associated with soil particles or aggregates.

1.3 Carbon stability

Multiple studies have been conducted in the last decades to understand the mechanisms responsible for carbon sequestration, which have led to multiple different conceptual models, making it difficult to establish policies based on these studies (Dynarski et al., 2020, Smith et al., 2020). The most direct way to increase soil carbon sequestration is to decrease the amount of carbon going out of the system by assuring its stability in soils. Carbon stability

refers to its resistance to decay by soil organisms (Dynarski et al., 2020). A good indicator of SOC stability is turnover time. This term refers to "the ratio of total carbon stock to output flux" (Sierra et al., 2017). In other words, turnover time is the time a given SOC stock would take to be exhausted if there were no C input.

Models developed before 2000 often separate soil organic carbon (SOC) in 2 to 5 different pools. Most of these models divide SOC in pools that are difficult to measure experimentally, such as an "active" pool, a "slow" pool, and a "passive" pool (Trumbore and Barbosa de Camargo, 2009). To separate SOC in measurable and physicochemically defined pools, Six et al. (2002) proposed 3 SOC stabilisation mechanisms: chemical stabilisation, physical stabilisation and biochemical stabilisation. Soil C that isn't protected by neither of those mechanisms is part of the so called "light fraction" (LF) and is often made of young organic matter. The model of J. Six thereby overcomes to the weaknesses of the previous models.

Chemical stabilisation is the result of organo-mineral associations between SOC and silt and clay particles (Conen et al., 2008; Zhao et al., 2006; Tan et al., 2007). The intensity of such protection can vary depending on the type of particle (Doetterl et al., 2015). Sesquioxides and silicate layers are the main surfaces capable of adsorbing organic matter (Krull et al., 2003). The most occurent sorption mechanism is the binding of negatively charged organic groups to particles through cation bridging. Therefore, the amount of chemical protection highly depends on the concentration in clay particles such as kaolinite or other aluminosilicates.

Physical stabilisation depends on soil aggregates, providing protection against biological activity. Those aggregates also develop organo-mineral associations with SOC, providing even more protection (Doetterl et al., 2015). Two types of aggregates can be experimentally separated and therefore studied separately: microaggregates (50 – 200 µm) and macroaggregates (> 200 µm). Doetterl et al. (2015) found that macroaggregates have a longer turnover time than microaggregates in a cropland in central Belgium, but carbon dynamics can differ depending on climatic conditions (Six et al., 2002). This could be explained by the fact that microaggregates can form within macroaggregates (Oades, 1984).

Finally, biochemical stabilisation, or recalcitrance, is related with the chemical composition of the organic carbon input. Complex molecules are likely to present longer decay times than others. However, this theory is debated as it has also been suggested that no organic molecule can be classified as intrinsically resistant to decomposition (Kleber, 2010; Schmidt et al., 2011, Dungait et al., 2012). From this point of view, recalcitrance depends on the microorganism population and thus, on the study conditions. However, molecules like fire-derived SOC, also called "char" have shown great general stability. Some argue that it is due to its recalcitrant composition (Knicker, 2007) while others propose that it is highly stable by contributing to microaggregate formation and, thereby, creating its own protection (Brodowski et al., 2006). However, even though uncertainties remain on which molecules are recalcitrant in which conditions, SOC chemical nature can explain part of its stability.

It is crucial to mention that environmental conditions, such as oxygen availability, soil temperature and moisture, have a major impact on carbon stability (Stockmann et al., 2013, Schmidt et al., 2011). Environmental conditions determine the activity potential of microorganisms and stabilisation mechanisms define how much organic matter is available for

mineralisation (figure 2). For example, buried C is generally more stable than topsoil C, partly because of the suboptimal environmental conditions (low oxygen availability) for microbial activity (Schmidt et al., 2011; Fontaine et al., 2007).

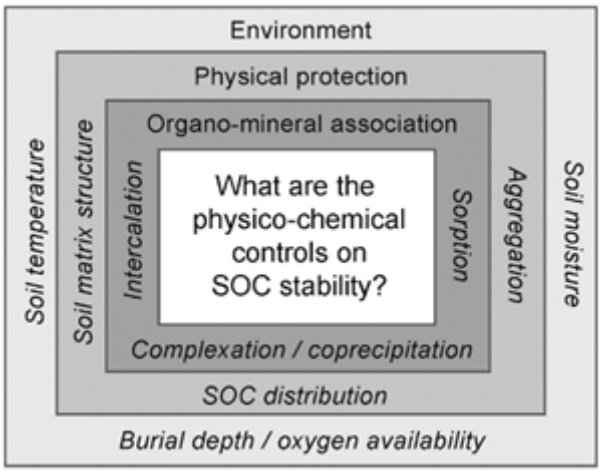

Figure 2: Factors influencing SOC stability (Doetterl et al., 2016). Environmental conditions determine microbial activity and stabilisation mechanisms (physical protection, chemical protection) determine the amount of available SOC for microbial activity.

1.4 Erosion

Soil erosion is a process in which soil particles are pulled and entrained to a new location. It is one of the biggest sources of soil degradation across the world (Kouli et al., 2009). Current agricultural practices have exposed soils to stronger erosion (Bollinne and Pissart, 1978). The main erosion vectors in temperate regions are water erosion caused by rainfall, wind erosion and tillage erosion.

In Wallonia, more than 40% of agricultural land is exposed to mean soil losses of 5 $tons.ha^{-1}.year^{-1}$ at least, regarding water erosion only. Silty soils of central Belgium are particularly exposed due to their texture and the concentration of weeded cultures such as potatoes, maïs and sugar beets[1]. Water erosion intensity depends on multiple factors such as rainfall intensity and slope length and percentage (Bollinne and Rosseau, 1978). Its intensity follows the revised universal soil loss equation (RUSLE) (Ghosal and Das Bhattacharya, 2020):

$$A = R * K * LS * C * P$$

Where A is the average soil annual loss $[t.ha^{-1}.year^{-1}]$, R is the rainfall erosivity factor $[MJ.mm.ha^{-1}.h^{-1}.year^{-1}]$, K is the soil erodibility factor $[t.h.MJ^{-1}.mm^{-1}]$, LS is the slope length and steepness factor [-], C is the cover management factor [-] and P is the conservation practice factor [-].

This equation considers that water erosion is directly correlated with the topography: flat high plateaus endure little or no erosion, erosion becomes more and more intense following the slope (with the increase of the LS factor) and soil particles settle at the bottom of the slope.

[1]Indicateurs clés de l'environnement wallon, SPW editions, 2012

Tillage erosion, presenting lower soil loss rates (mostly between 0.4 and 0.8 $tons.ha^{-1}.year^{-1}$ in mechanized agriculture), have received less attention than other types of erosion (Van Oost et al., 2006). However, it is now proven that tillage erosion is a major soil degradation process (Heckrath et al., 2005). Moreover, it can amplify water erosion by infilling rills and thus, increasing runoff (Wang et al., 2016). Tillage erosion results in a net translocation of soil from convex landscape positions to concave landscape positions. Thus, tillage erosion and water erosion can have convergent effects at certain positions and divergent effects at others (figure 3).

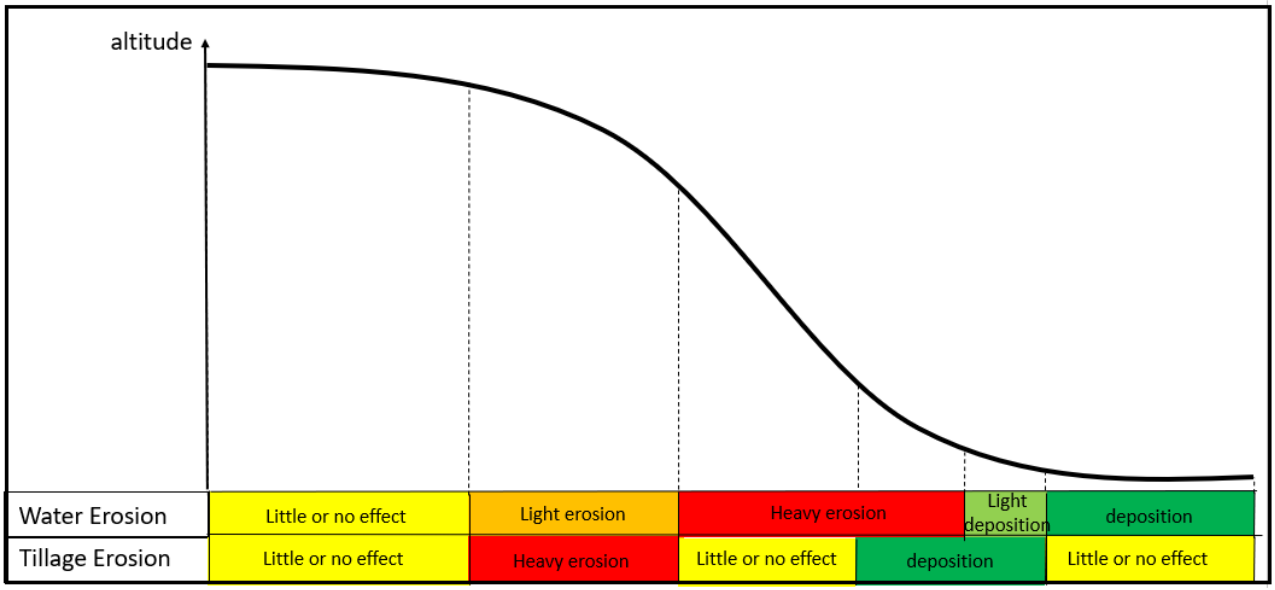

Figure 3: Effects of water and tillage erosion along the slope profile. Even though the same colour scale is used for both processes, water erosion rates are 5 to 10 times larger than tillage erosion rates in the study area's region (central Belgium).

1.5 Erosion and carbon stability

The focus of this work is to determine whether water and tillage erosion have an impact on carbon stability. In other words, does erosion represent a source of C emissions or a C sink? Studies during the 2000's have led to different conclusions, depending on the studied landscape element and time scale (Doetterl et al., 2016). However, some known impacts of erosion on carbon dynamics can already be highlighted (figure 25).

Firstly, heavy erosion exposes former subsoil layers to the surface, changing their environmental conditions and facilitating the decomposition of SOC that was strongly protected before. The breakdown of aggregates by water erosion also lowers the SOC stability (Six et al., 2000). Secondly, addition of fresh labile C to older C stocks is likely to diminish the turnover time of the latter. This can be explained by the fact that new C is an easy energy source for decomposers, which allows the microbial population to grow (Fontaine et al., 2007). However, former subsoil layers are very likely to have a lot of non-C-saturated minerals, capable of fixing transported SOC coming from higher slope locations or fresh organic matter. Therefore, we talk about "dynamic replacement of eroded C", making it possible for

little to moderate erosion intensities to be a C sink (Doetterl et al., 2016). It is important to notice that water erosion preferentially transports soil particles enriched in fresh organic matter (Kuhn, 2007). Thus, erosion locations mainly loose C-rich sediments but unstable SOC.

Erosion cycles also have an impact on carbon stability at deposition locations. Those locations must be studied with interest because they contain between 70% and 90% of transported SOC during water erosion processes, the remaining part going to lakes or oceans via river systems (Doetterl et al., 2016). It is even truer for tillage erosion, in which transport of soil particles and associated SOC take place on a very limited geographical scale: from a convexity to the nearest concavity. Once transported to deposition locations, SOC is buried to deeper soil layers where it has a priori greater stability. Nevertheless, most studies focused on the first 30 cm of soil, making it extremely difficult to precisely establish the stability of buried SOC coming from sediment transport (Doetterl et al., 2016). A greater SOC content also allows aggregates to form, enhancing carbon stability at deposition locations.

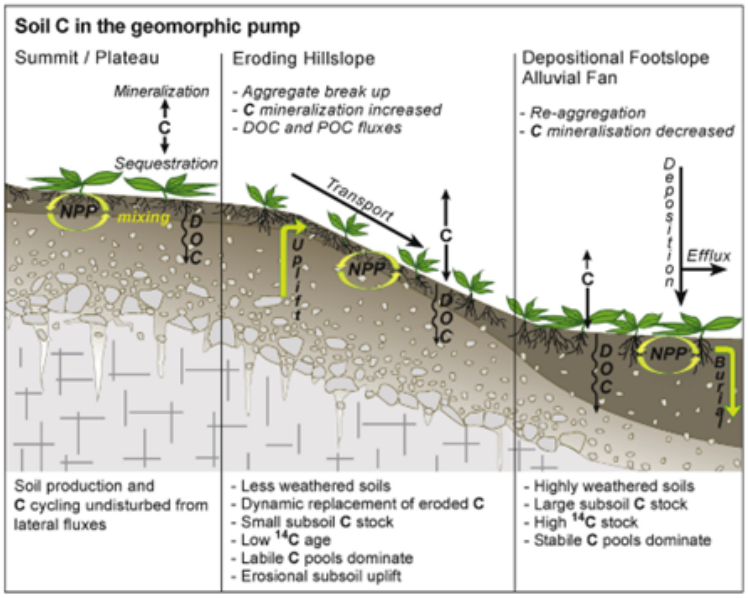

Figure 4: Impact of erosion, transport, and deposition processes of water erosion (Doetterl et al., 2016). SOC distribution on plateaus is simply regulated by a balance of inputs and mineralisation. On eroding landscapes, soil is altered, aggregates are broken down and subsoils are brought back to surface and part of SOC is transported. The loss of C allows a better fixing of new fresh C inputs (dynamic replacement). At deposition landscapes, SOC is buried, and soil aggregates are reformed.

Uncertainties remain in multiple stages of the erosion-transport-deposition cycle (Polyakov and Lal, 2004). For example, the fate of SOC during the transport phase is very poorly known. Moreover, erosion has a major impact on soil properties such as structure, which itself has impact on SOC stability, but few studies have focussed on this relation. Concerning tillage erosion, studies have shown its impact on SOC distribution (Van Oost et al., 2005) but its impact on SOC stability remains unclear.

1.6 Objectives

As shown in the previous sections, multiple studies have contributed to a better understanding of SOC stability and its link with erosion. However, they have also highlighted the remaining uncertainties, which are partly addressed in this work. The particularities of this study are the quantification of carbon stability at different locations along the topographic profile, the linking between SOC stability and multiple other SOC properties, and the additional focus on the effects of tillage erosion, not only on SOC distribution but also on SOC stability. The objectives are formulated as follow:

1. Compare carbon stability at different topographic locations in order to establish the potential impact of water and tillage erosion.
2. Establish on which carbon stabilisation mechanism water and tillage erosion act or not by comparing SOC properties at different topographic locations.
3. Give an estimation whether water and tillage erosion represent a carbon sink or source at the scale of one field.

2 Material and methods

2.1 study site description

The study has been conducted on a field in Orp-Jauche (figure 5), in central Belgium. Two main reasons explain the selection of this location: (i) it presents, within the same field, multiple and pronounced topographic situations and (ii) the erosion intensity had already been estimated during the year 2022 by Pierre Baert during his master thesis. This work provided valuable data and made it possible to establish a sampling design and to launch measurements early. The field has a surface of 15.29 ha and can be schemed as a diamond with its extremities at the four main cardinal points. Roads border the N-E, E-S and S-W sides. The W-N side is bordered by another field which is separated from the study field by a small grass line and a ditch. According to the measurements established by the *Royal Institute of Meteorology*, the mean annual temperature at Orp-Jauche between 1991 and 2020 is 10.5°C and the mean annual precipitation quantity for the same period is 758 mm.

Figure 5: satellite view (orthophotoplan 2020) of the study field (WalOnMap)

Following the numeric map of Walloon soils, the study field is characterized by a silty texture and favourable drainage in its totality. Indeed, Orp-Jauche is situated in the silt-loam belt of central Belgium, where soils develop on geological loess deposition. The erosion sensitivity of soils located on this belt are particularly high, due to their texture and the wide presence of erosion-sensitive cultures (Bielders et al., 2003). The profile development can vary within the field, going from a textural B horizon on the E-S and S-W sides to an absence of profile development in the middle of the field and on the W-N side. A mix between a textural and structural B horizon can also be found, mainly on the N-E side.

The parcel is managed with conventional cultivation techniques. Initially, the actual field was separated in multiple patches before being progressively regrouped in one field due to reparcellings between 1971 and 2006 (appendix I). However, all the initial parcels seem to have been managed following the same cultivation techniques. The actual crop rotation consists of an alternance of sugar beets, winter wheat, potatoes, and vegetables. No or little organic amendment are brought by the cultivator. Over the season 2022-2023, the study field is growing 3 different varieties of winter wheat in order to product wheat seeds.

As mentionned previously, the study location has been chosen mainly for its topographic characteristics (figure 6). The difference between the highest and lowest point is 19.75 m. High grounds are situated on the E-S and S-W sides. Two main water run-off axes can be found and meet up at the northern extremity of the field, where all the watershed streams converge in a tunnel going under the road. The first run-off axe borders the W-N side and gather the streaming from the western part of the study field and from other fields nearby. The second one links the southern high ground to northern extremity of the field. Some smaller run-off axes also gather a part of the streaming before combining with the main ones. The most notable secondary axe links the eastern quarter of the field to the middle of the field where it joins a larger run-off axe.

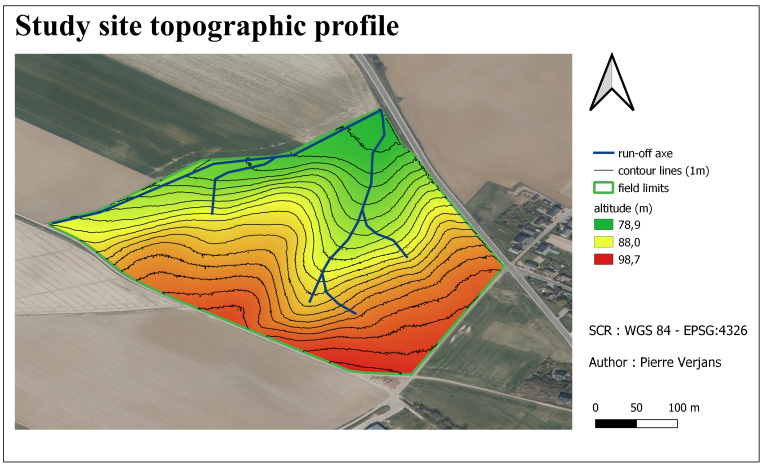

Figure 6: topographic profile of the study field

2.2 Samplign design

Six erosion scenarios have been identified while combining the effects of hydric and labour weathering or deposition (figure 7). The first plot, plateau (P), is characterized by little or no effect by neither erosion modalities and used as a control scenario. Four other scenarios can be separated in two groups: erosion scenarios on the convex plot (X) and the slope plot (S) on one hand, and deposition scenarios on the concave plot (A) and at the bottom of the slope (B) on the other hand. A last scenario is called “opposite effects” (O) and is characterized by labour deposition and water erosion.

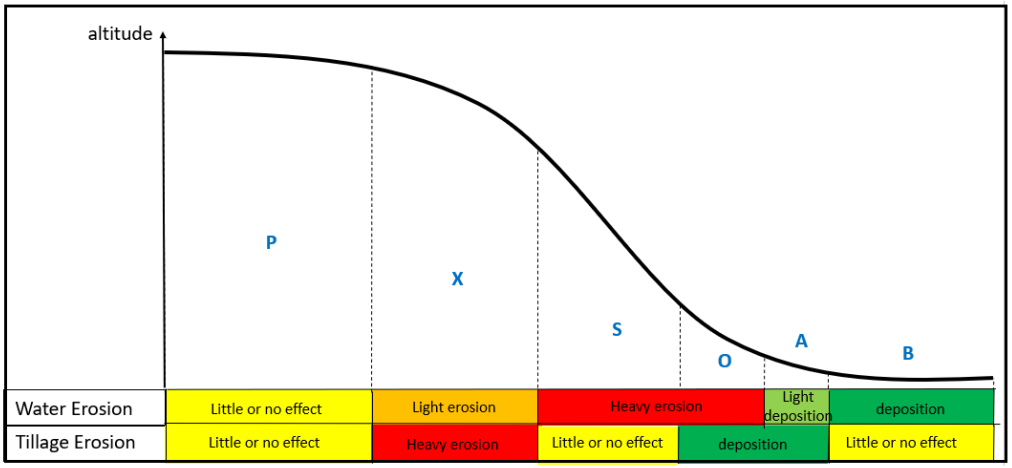

Figure 7: theoretical position of the 6 experimental plots along the slope

The plots P, S, A and B are placed on an approximatively straight line connecting P, in the southern part of the studied parcel, to B, at the northern end of the parcel. Both points are on a flat terrain at the top and bottom of the slope profile respectively. S is located around the steepest slope of this toposequence and A around the most pronounced concavity. O is placed near but east of this line, so it is simultaneously on a slope of a secondary run-off axe, and on a concavity following a slope profile going from east to west. X is placed on another hillside where convexity is more expressed but where the slope is less intense.

The plots localisation (figure 8) have been determined by observing slope profiles (figure 9) based on the digital terrain model of Wallonia established in 2013-2014 (WalOnMap), and with the estimations of labour and hydric erosion or deposition, with a resolution of 20x20m, calculated by the WaTEM/SEDEM model (appendix C). Those estimations have been performed by Pierre Baert during his master thesis at Gembloux Agro-Bio Tech in 2022. A particular attention has also been put on avoiding the edges of fields before the reparcelling, where heavy organic matter deposition such as manure piles could have taken place (appendiw I. With the field growing 3 different winter wheat varieties (appendix D), plots are not rigorously supporting the exact same crop. Plot P, X, A and B are sown with variety 1 and plot S and O are sown with variety 2.

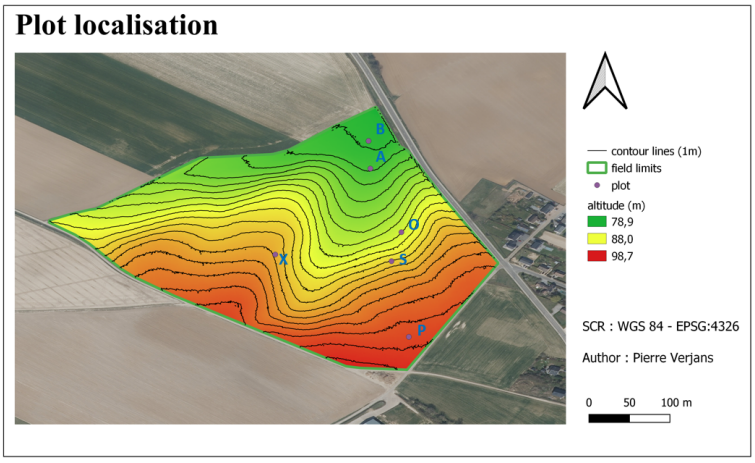

Figure 8: localisation of the experimental plots on the study field

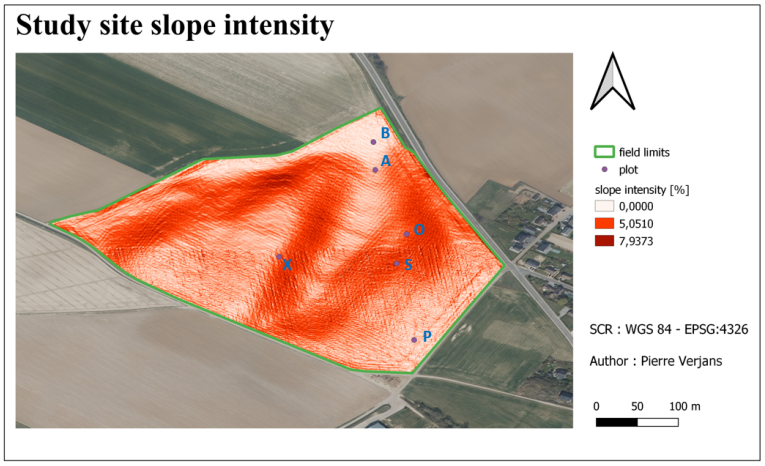

Figure 9: slope intensity and plot localisation on the study field

2.3 Plot characterisation

Each plot consists of 5 white collars for soil CO_2 fluxes measurements, 4 root auger points and 1 classic auger point (figure 10). White collars are disposed 80 cm apart in a cross with a collar in the middle of the plot. Root auger points are made at a 1m distance of the middle of the cross, and in four perpendicular directions. Finally, the classic auger point is made slightly further than the root auger points. The purpose of each of those experimental devices is explained in the following sections.

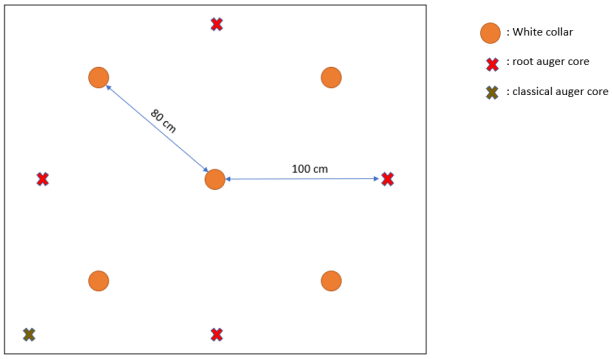

Figure 10: design of an experimental plot

In order to better understand the system and the differences between the experimental plots, multiple measurements have been realised. The 4 root auger cores have a critical role in the characterisation of all the plots. This auger allows to take a defined volume of soil without altering its structure. One soil core was made from 5 layers of 10 cm, each layer forming a soil sample. Those samples were weighted fresh and a fraction of it (around 100g) was taken to constitute a subsample. Subsamples were weighted fresh before being air-dried at 40°C and then weighted dry. They were also crushed and sieved at 2mm before being kept in a fridge at a temperature around 5°C to inhibit microorganism activity and, thus, carbon mineralisation. The difference between fresh and dry mass was used to calculate the water content of each sample, assuming that subsample water content and sample water content are equal. Knowing each sample volume, wet mass and water content, soil bulk density is calculated for each

sample with the following equation:

$$rho = \frac{M_{wet} - (M_{wet} * \frac{WC}{100})}{V}$$

Where rho [g/cm^3] is the sample soil bulk density, Mwet [g] is the mass of the fresh soil sample, WC [%mass] is the subsample water content and V [cm^3] the root auger volume. Note that Mwet * WC is the mass of water inside the fresh sample. Soil bulk density is calculated for each sample and a mean density is calculated for each depth at a same plot (n=4) for further calculations.

Subsamples were then used for further soil analysis. For each manipulation, a part of the subsample was taken. The first of these measurements was the estimation of the carbon total stock of each plot. It was made by measuring the carbon content of each subsample by dry combustion. This technique consists in heavily heating (around 1000 °C) the soil sample, resulting in the complete oxidation of organic carbon into CO_2. Measuring the amount of CO_2 released during the process gives the amount of C initially situated in the soil sample. This measurement has been conducted by the provincial centre of agriculture and rurality at La Hulpe. The SOC stock of each sample was calculated with the soil bulk density measured for this sample, the SOC content measured by dry combustion and the sampling thickness (= 10 cm) following the equation:

$$SOC_{stock} = rho * SOC_{content} * d$$

Where SOCstock [kgC/m^2] is the amount of soil carbon in a layer of 10cm by surface area, rho [kgsoil/m^3] is the mean soil bulk density of the 4 samples (same plot and same depth) previously calculated, $SOC_{content}$ [kgC/kgsoil] is the mean carbon content of the sample measured by dry combustion and d [m] is the hight of the root auger. The SOC_{stock} equation is applied on each 10cm layer for each soil core. A depth distribution of SOC_{stock} is established for each plot by averaging SOC_{stock} of the 4 samples at each sampling depth. Additionally, a total SOC_{stock} is calculated for each soil core by summing the SOC_{stock} of the five layers. The mean SOC_{stock} of the 4 soil cores is considered to be the SOC_{stock} of the entire plot for further calculations.

Besides the 4 root auger samplings, one classical auger sampling to a depth of 80cm was made for each plot. This sampling was made to establish the pedologic profile of each plot and to check the validity of the information brought by the numeric map of Walloon soils. Finally, nitrogen in were measured for the 4 topsoil samples of each plot in order to establish topsoil C/N ratios.

2.4 Soil CO_2 fluxes measurements

Soil CO_2 flux (Fs) measurements give a good approximation of SOC global stability. Indeed, measured CO_2 fluxes through time put in relation with the total SOC_{stock} give the mineralisation rate of each plot. As a reminder, the mineralisation rate of a SOC_{stock} is the proportion of this stock which is mineralised by soil organisms in a given time.

In order to measure these fluxes, 5 white collars were fixed on each plot by pressing the lower bottom of the white collars 10cm deep into the soil. The white collars are dimensioned

to receive a SCR-2 respiration chamber (area of $78cm^2$), connected to a portable CO_2 gas analyser EGM-5. The gas analyser contains an infrared gas analyser (IRGA) cell (figure 11). The air from the gas chamber steams in (gas in) and out the cell (gas out). At one end of the cell, an infrared source emits a certain amount of energy at a particular wavelength, for which CO_2 molecules present an absorption band. At the other end of the cell, a detector measures the amount of energy reaching the end of the cell. The difference between the emitted and received energy depends on the concentration of CO_2 in the cell and, by extension, in the gas chamber.

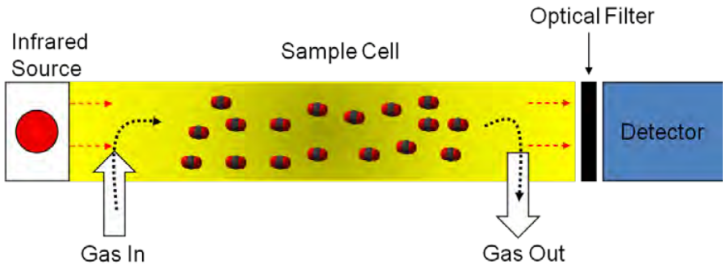

Figure 11: principle of an IRGA cell

Due to the adequate dimension of the white collars, the gas chamber and the soil surface create a closed system wherein CO_2 increases are the result of soil fluxes, regrouping SOC mineralisation by micro-organisms and root respiration. White collars were placed two weeks before the beginning of the experiment to stabilize the system before any measurement. Plants inside the white collar and eventual later emerging sprouts were cut and removed out of the system on this day and before any measurement. This precaution limits the part of root respiration on the total soil CO_2 flux. However, the development of roots by plants nearby the white collars certainly does not stop at the collar limits. Figure 11 gives a visual indication of the root development at the end of the study period in the top 10cm of the soil underneath the white collars.

Figure 12: roots in the topsoil (first 10cm) underneath a white collar at the end of the study period.

For each measurement, the CO_2 concentration above one white collar was observed for six consecutive minutes. The concentrations at minutes 0, 1, 2, 3, 4, 5 and 6 were noted. The calculation of F_s is inspired by the work of Maier et al. (2011). A linear regression is established, relating the concentration values to time. If the linear regression is close enough from the measured data ($R^2 > 0.95$), the regression coefficient is considered as the F_s of the sample (n=5 per plot and per measurement day). If not, the concentration at minute 0 is withdrawn from the linear regression and if R^2 is still higher than 0.95, value at minute 6 is withdrawn. Indeed, soil flux can take some time to stabilise (first minute of measurement) and, at high concentrations in the gas chamber (at the end of the measurement), CO_2 diffusion from soil to the gas chamber can be slowed down by the decrease of the concentration gradient. The mean of F_s from the 5 samples is considered as the F_s of the plot at a certain day. 11 flux measurements were conducted from the 29/3 to the 11/7, for a total period of 104 days (figure 13).

Soil fluxes are initially measured in [ppm/min]. A more common unit in literature is $[mol.m^{-2}.s^{-1}]$. Therefore, a conversion needs to be done with the following equation:

$$F_s = F_{s,ppm} * \frac{1}{60} * \frac{1}{22.414} * \frac{V}{A} * 1000$$

Where Fs is the soil CO_2 flux in $[\mu mol.m^{-2}.s^{-1}]$, $F_{s,ppm}$ is the soil CO_2 flux in [ppm/min], 1/60 is the conversion factor from $[min^{-1}]$ to $[s^{-1}]$, 22.414 is the ideal gas constant at standard pressure and temperature [L/mol], V is the the gas chamber volume $[m^3]$, A is the surface of the white collar $[m^2]$ and 1000 is the conversion factor from [L] to $[m^3]$.

In order to quantify C stability, soil fluxes must be expressed as a flux of C relative to the total amount of soil C at the studied plot. As mentioned in the section 2.3, a SOC_{stock} has been calculated for each plot. The conversion from $[\mu mol.m^{-2}.s^{-1}]$ to $[mgC.gCsoil^{-1}.hr^{-1}]$ is done in two steps. The following equation converts $[\mu mol.m^{-2}.s^{-1}]$ into a mass of C per hour $[mgC.m^{-2}.hr^{-1}]$.

$$F_{s,mass} = F_s * Mc * 10^{-3} * 3600$$

Where $F_{s,mass}$ is the soil CO_2 flux in $[mgC.m^{-2}.hr^{-1}]$, Mc is the molar mass of C [g/mol], 10^{-3} is the conversion factor from [g/mol] to [mg/μmol] and 3600 is the conversion factor from $[s^{-1}]$ to $[hr{-}1]$. The following equation then converts a surface of ground into an amount of ground C.

$$F_{s,rel} = F_{s,mass} * SOC_{stock}^{-1} * 10^{-3}$$

Where Fs,rel is the soil C mineralisation rate $[mgC.gCsoil^{-1}.hr^{-1}]$, SOC_{stock} is the C stock of the study plot [kgC/m^2] and 10^{-3} the conversion factor from $[kgC^{-1}]$ to $[gC^{-1}]$.

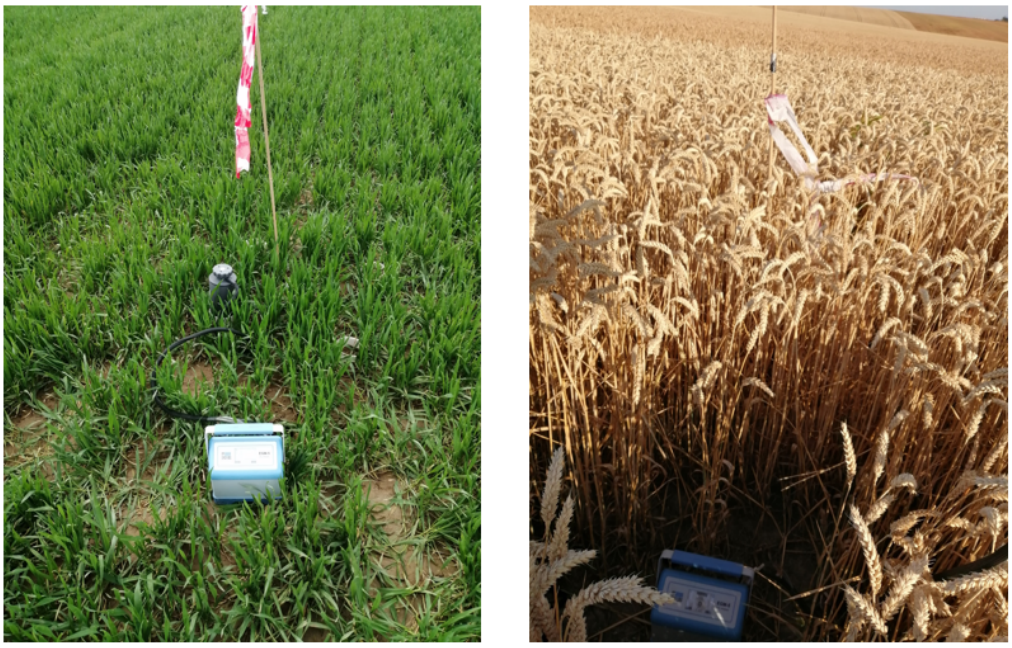

Figure 13: EGM5 and respiration chamber setup at day 0 (left) and at day 104 (right).

2.5 Walkley and Black carbon quantification

In addition to the carbon quantification by dry combustion, another carbon quantification method has been applied on the same samples. The Walkley and Black method is an easy and relatively quick way to quantify soil organic carbon contents and is therefore one of the most frequently used methods (Meersmans et al., 2009). It relies on the oxidation of organic C by potassium dichromate in a strongly acidic medium. However, this method, unlike the dry combustion method mentioned earlier, underestimates the soil organic carbon content. Indeed, the attack can only reach "readily oxidable C" (Sato et al., 2014). Some recalcitrant carbon forms such as charcoal (De Vos et al., 2007 ; Conyers et al., 2011) or organic carbon highly protected in aggregates (Sato et al., 2014) are not oxidized by potassium dichromate. Generally, a correction factor, most commonly 1.33, is applied to the measured carbon content

to obtain the real carbon content (Meersmans et al., 2009). However, in this study no correction factor is applied during carbon content calculations. Walkley and Black results are then compared to dry combustion results in order to calculate a recovery factor for each sample and study the potential differences between the six study plots. The recovery factor is the % of carbon detected by dry combustion that is also detected by the Walkley and Black method.

The first phase of the Walkley and Black method consists in the oxidation of organic C. This is performed by reduction of Cr^{6+} to Cr^{3+} in presence of a strong acid. The quantity of potassium dichromate is greater than the requested quantity to oxide the organic carbon present in the 1g soil samples.

$$2K_2Cr_2O_7 + 8H_2SO_4 \longrightarrow 2K_2SO_4 + 2Cr_2(SO_4)_3 + 8H_2O + 3O_2$$

$$3C + 3O_2 \longrightarrow 3CO_2$$

The excess of dichromate potassium is then titrated with a Mohr's salt solution in presence of a colour indicator, diphenylamine (figure 14). The titration follows the following reaction.

$$K_2CR_2O_7 + 6Fe(NH_4)_2(SO_4)_2 + 7H_2SO_4 \longleftrightarrow Cr_2(SO_4)_3 + 7H_2O + 6FeNH_4(SO_4)_2 + K_2SO_4 + 3(NH_4)_2SO_4$$

The amount of Mohr's salt needed for the titration gives the quantity of excessive potassium dichromate. A blank sample is also used to get the exact initial quantity of potassium dichromate. Due to its high sensitivity to degradation through time, the concentration of the Mohr's salt solution was verified before every series of sample by titrating two times 50mL of a strictly known solution of potassium dichromate in presence of sulfuric acid. The soil carbon content is calculated following the equation:

$$SOC_{content} = 18 * \tfrac{1}{6} * (V_{bl} - Vs) * C_{MS} * m^{-1}$$

Where $SOC_{content}$ designs the SOC content [gC/kg] of the measured sample, 18 is the mass of oxidised C per used mole of dichromate potassium [gC/mol], (1/6) is the amount of dichromate potassium titrated by one mole of Mohr's salt [mol/mol], V_{bl} and Vs are the volumes of Mohr's salt solution [L] needed to titrate the blank sample and the soil sample respectively, C_{MS} is the concentration of the Mohr's salt solution [mol/L] determined by the concentration verification and m [kg], the mass of the soil sample.

Figure 14: Titration of dichromate potassium excess by Mohr's salt.

2.6 Soil fractionation

After studying the impact of erosion on biochemical stabilisation mechanisms, soil fractionation has been used to investigate potential impacts on chemical or physical stabilisation mechanisms. Many different soil fractionation protocols have been developed in the literature. Some separate particulate organic matter (POM) from SOC chemically bonded to silt and clay particles (Gavinelli et al., 1995). Other protocols separate SOC physically protected inside aggregates from the rest of SOC (Six et al., 1998). Each carbon fraction is associated to a certain degree of stability, some studies even measure the mean age of each C fraction.

The protocol followed for this report in based on the works of Balesdent, Feller and Gavinelli (Balesdent, 1991 ; Feller, 1994 ; Gavinelli et al., 1995). This method is based on a granulometric separation of different soil fractions. Soil samples are divided into three fractions: 200-2000 μm particles, 50-200 μm and smaller than 50 μm particles. The two fractions containing the largest particles mainly contain relatively fresh POM, which has been only slightly transformed by microorganisms. This type of SOC is called "light fraction" (LF). The 50-200 μm fraction contains slightly more transformed organic matter than the larger fraction. The smallest granulometric fraction contains the SOC that is chemically bonded with soils particles. This C is called "heavy fraction" (HF). It includes organic C bonded with silt and clay particles and organic C that is protected inside aggregates (Six et al., 2000).

To give an indicator of the stability of each fraction, the French national institute for agronomic research (INRA) measured the mean carbon ages of the three different soil fractions for silty cultivated soils: respectively 3, 12 and older than 50 years. It is important to underline the fact that this protocol can only highlight heavy fraction with no distinction between physically and chemically protected carbon. That is because, aggregates are at least partially dismantled in multiple smaller particles bounded with organic matter, and, to a smaller degree, in larger organic matter pieces.

The protocol applied here consists in the following manipulations. 40g of previously crushed and dried soil samples are put in a solution of Sodium hexametaphosphate 0,25% and agitated at 5 Hz frequency for 2 hours. This step puts the soil particles in suspension

and breaks down the aggregates. The solution is then put through a 200 μm and a 50 μm mesh. Each mesh is rinsed multiple times with distilled water. The water charged with the smallest particles is collected into a beaker. The two meshes are backwashed with distilled water and the particles are collected into two separate beakers. Water is then evaporated in stove at a temperature of 60 °C. Finally, fractions are collected and their carbon content is measured by dry combustion. Due to the difficulty to rigorously collect the entire fraction, beakers are weighted before the manipulation. The mass of each fraction is calculated by the difference between the beaker weight before and after the manipulation. The carbon content of each fraction is multiplied by its mass, giving the repartition of total carbon between the 3 fractions.

Due to time and logistic limitations, soil fractionation has been conducted only on samples of the topsoil (first 10cm) and for only three plots: plots P, S and B. Indeed, the quantity of laboratory material was limited, the water evaporation takes several days, and dry combustion analyses take slightly more than a month. Topsoil has been chosen in priority over deeper samples to observe potential impact of erosion on the horizon where it most directly affects soil structure. Plots P, S and B were chosen to have a complete observation of erosion-transport-deposition cycle for water erosion instead of partial observations for water and tillage erosion. With the assumption that higher erosion rates go along with higher impacts on SOC stability, water erosion has been arbitrarily prioritised over tillage erosion because its erosion rates are likely much higher than tillage erosion rates on the study field. The three other plots are currently undergoing dry combustion analyses at the provincial centre of agriculture and rurality at La Hulpe and results should arrive in early-september.

2.7 Temperature and moisture measurements

As mentioned in section 1.2, environmental conditions have a critical impact on microbial activity and thus, on SOC mineralisation. Therefore, it is necessary to verify potential differences in environmental conditions between plots before drawing conclusions about the effects of other parameters on C stability. At the same time CO_2 fluxes were measured, abiotic parameters of each plot were gathered. To that end, a 5TM sensor was introduced less than 10 cm from each white collar (figure 15), giving topsoil moisture and topsoil temperature values. The plot moisture and temperature were calculated by averaging all measures (n=5).

Figure 15: 5TM sensor introduced next to a white collar.

The 5TM sensor calculates soil water content from measuring the dielectric permittivity, which is directly correlated with moisture, of the soil wherein it is placed. However, the exact relation between soil moisture and soil dielectric permittivity depends on soil texture and soil bulk density. Therefore, the sensor needs to be calibrated in the conditions studied. For this study, the calibration has been performed in a typical loess belt soil of central Belgium, and at the mean soil bulk density of all the 0-10cm samples (=1.7 g/cm^3). The 5TM sensor was inserted in 6 different soil moistures values (fig 16) to obtain a linear equation linking raw sensor measurements to soil moisture. The obtained equation is then used to convert field data into soil moisture values.

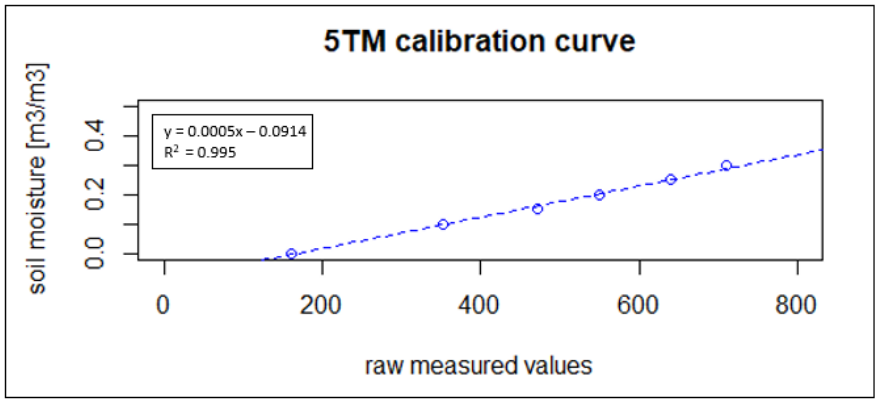

Figure 16: Calibration of the 5TM sensor. Points indicate the measured values used to establish the equation.

2.8 Methodological approach

The previously explained measurements result in multiple data sets that need to be combined in order to respond to the study objectives (figure 17). Although it strictly speaking gives no information on SOC stability, the SOC total stock (SOC_{tot}) for each plot is a key data. As a reminder, SOC_{tot} is the mass of C contained in the top 50cm. Indeed, Walkley and Black measurements are compared to it to quantify the amount of recalcitrant carbon. Moreover, Fs are put in relation with SOC_{tot} to calculate mineralisation rates [$mgC.gCsoil^{-1}.hr^{-1}$]. This value is the most direct quantification of SOC stability. Measurements of environmental conditions, recalcitrant C and C distribution within soil fractions are made to find potential factors explaining C stability differences along study plots. SOC_{tot} is calculated on base of two measurements: SOC content and soil bulk density.

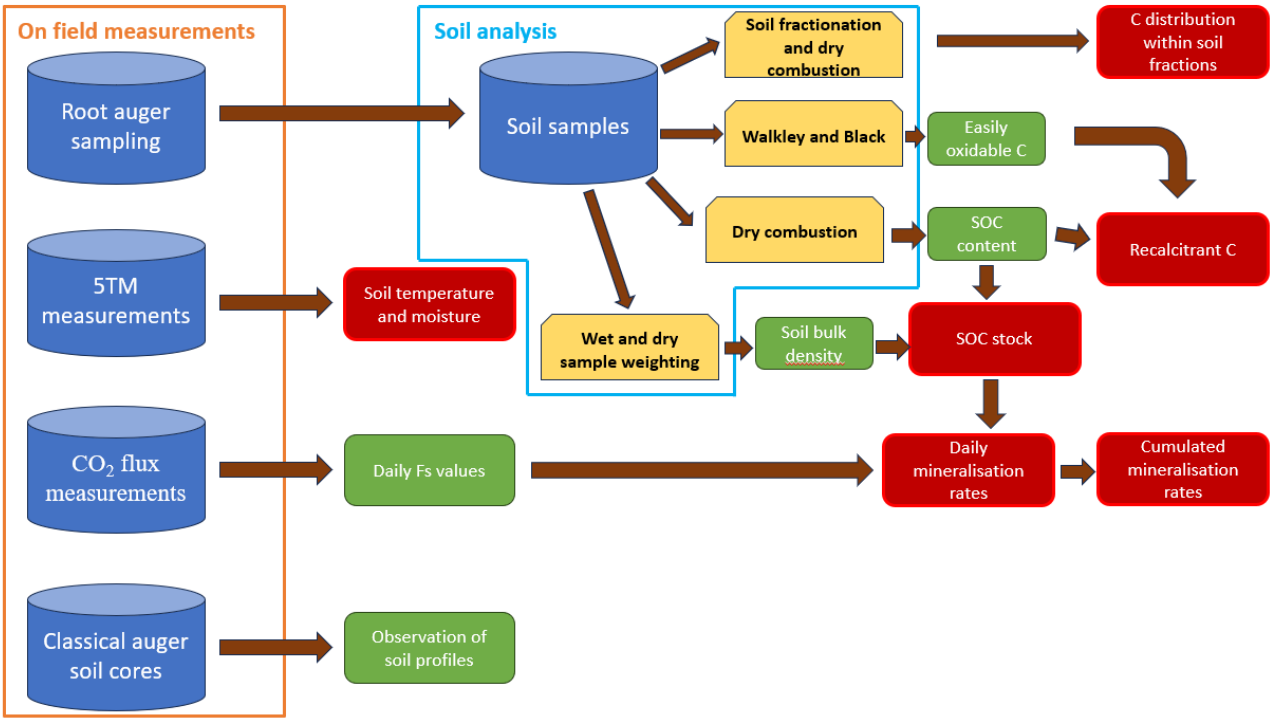

Figure 17: Methodological flowchart. Values in red are used to quantify or explain soil C stability differences between plots.

2.9 Soil flux modelling

Multiple models have been implemented to predict soil CO_2 fluxes from different parameters. Recently, machine learning models have been developed to predict F_s based on parameters such as soil classification, soil temperature, and soil moisture (Adjuik and Davis, 2022). Nevertheless, much simpler models do exist, using a relation between soil temperature (T) and F_s.

The model tested in this study is the Q10 model. This model relies on a Q10 parameter which translates the sensitivity of F_s to temperature changes. Its value is equal to the multiplication of F_s for a 10°C temperature increase (Meyer et al., 2018). To calculate this parameter, an exponential regression is established between measured temperatures and measured F_s. The equation of this regression takes the form of equation (i). The parameter b of this equation is then implemented in the equation (ii) to find the value of Q10. A Q10 value is calculated for each white collar and the mean of the 5 values is considered the Q10 of the plot. In this study, the Q10 model is used to quantify the temperature sensitivity of each plot. Therefore, a comparison between the Q10 values for each plot has been made.

$$F_s = a * e^{bT} (i)$$
$$Q10 = e^{10*b} (ii)$$

Where F_s is the soil CO_2 flux $[mgC.gCsoil^{-1}.hr^{-1}]$ and T the measured temperature [°C]. F_s values are then interpolated from measured temperatures following the equation:

$$F_s = F_{ref} * Q10^{\frac{T-T_{ref}}{10}}$$

Where F_{ref} is the soil CO_2 flux $[mgC.gCsoil^{-1}.hr^{-1}]$ at the reference temperature T_{ref}

[°C]. For this study, T_{ref} has been fixed at 10°C to translate the basal soil respiration, since annual mean temperature at Orp-Jauche between 1991 and 2020 is 10.5°C (Royal Institute of Meteorology). In addition, the root mean squared error (RMSE) was calculated for each model (one model per plot) between predicted values and mean measured values for the measurement days.

2.10 Statistical analyses

Statistical analyses were operated on R 4.1.2. To highlight possible significant differences between plots, statistical tests were applied on C content at each depth, soil bulk density at each depth, SOC stock at each depth, total SOC stock, C/N ratio, cumulated mineralisation, recovery rate for Walkley and Black method, part of C found in the heavy fraction and soil temperature and moisture.

Before applying each of these statistical analyses, the normality of the data was tested with a Shapiro-Wilk test and the homogeneity of variance amongst the six plots was tested with a Levene test. If the null hypothesis of population normality and variance equality between populations were not rejected, a one-way anova (ANOVA1) was performed. If not, a non-parametric KRUSKAL-WALLIS test was used (table 1). For measurements where the number of samples per plot (n) was inferior to 10, the assumption was made that normality was respected.

In case of significant differences being found between plots, a post-hoc test was applied to class the means in significantly different groups. Therefore, a Tukey or a Dunn pair-wised comparison were used respectively after a ANOVA1 or a KRUSKAL-WALLIS test.

Table 1: statistical tests applied on each of the measurements.

Measurement	replicates (n)	Test
C content per depth	4	ANOVA1
Soil bulk density per depth	4	ANOVA1
SOC stock per depth	4	ANOVA1
Total SOC stock	4	ANOVA1
C/N ratio	4	ANOVA1
Cumulated mineralisation	5	ANOVA1
Recovery rate by WB	20	KRUSKAL-WALLIS
Soil C fractions proportion	4	ANOVA1
Temperature	55	ANOVA1
Moisture	55	KRUSKAL-WALLIS
Q10 values	5	ANOVA1

3 Results

3.1 Plot characterisation

The results of plot characterisation at the different plots corresponding to the 6 erosion scenarios (figure 7 in section 2.2) are given below. Reported are the carbon content, the soil bulk density and the SOC stock, evaluated by using the dry combustion results and the sample weighting. The quantification of N also allowed to establish C/N ratios for every topsoil sample.

3.1.1 Carbon content

Table 2: mean carbon content measured by dry combustion at study plots and at 5 different depths associated with their standard deviation. Letters indicate the groups determined by a post-hoc tukey pair-wise comparison ("a" class is systematically allocated to the highest value group).

	Soil C content [gC/kgsoil]					
depth	P	X	S	O	A	B
0-10cm	10.46 ± 0.45 b	9.21 ± 0.62 b	11.31 ± 1.37 b	11.98 ± 0.54 a	14.14 ± 1.46 a	12.62 ± 2.05 a
10-20cm	10.31 ± 0.89 b	9.19 ± 0.40 b	10.43 ± 0.53 b	12.87 ± 1.51 a	13.61 ± 1.46 a	11.40 ± 0.92 a
20-30cm	11.16 ± 2.67 a	5.59 ± 2.17 b	5.34 ± 0.77 b	11.15 ± 0.76 a	13.26 ± 2.78 a	12.28 ± 0.71 a
30-40cm	4.39 ± 0.56 c	2.56 ± 0.42 c	4.69 ± 1.67 c	8.94 ± 1.51 b	10.51 ± 0.72 ab	12.53 ± 2.98 a
40-50cm	3.83 ± 0.37 bc	3.13 ± 1.48 c	3.97 ± 0.33 bc	5.41 ± 0.46 b	10.31 ± 0.96 a	9.86 ± 0.24 a

Dry combustion C quantification (table 2) showed significant differences in carbon content between study plots. Results show that control and erosion plots (P, X and S) have smaller carbon contents than the 3 other plots at 0-10cm and 10-20cm depths. Carbon contents at X and S start decreasing at depth 20-30cm where their carbon contents are significantly lower than all the others. At depth 30-40cm, carbon content at plot P and O also starts decreasing. Plots A and B maintain a significantly higher carbon content at 30-40cm and 40-50cm. Carbon content at plot O decreases less at lower depth than carbon content at plot P, X and S. Appendix A gives a graphical representation of depth carbon content distribution at each plot.

3.1.2 Soil bulk density

Table 3: mean soil bulk density at study plots and at 5 different depths associated with their standard deviation. Letters indicate the groups determined by a post-hoc tukey pair-wise comparison ("a" class is systematically allocated to the highest value group).

	Soil bulk density [g/cm^3]					
depth	P	X	S	O	A	B
0-10cm	1.81 ± 0.10	1.68 ± 0.04	1.66 ± 0.17	1.67 ± 0.05	1.71 ± 0.07	1.64 ± 0.05
10-20cm	1.76 ± 0.23	1.86 ± 0.18	1.70 ± 0.09	1.63 ± 0.12	1.89 ± 0.09	1.91 ± 0.17
20-30cm	1.82 ± 0.24 ab	1.77 ± 0.10 ab	1.57 ± 0.08 b	1.91 ± 0.10 a	1.72 ± 0.10 ab	1.71 ± 0.10 ab
30-40cm	2.03 ± 0.01 a	1.78 ± 0.10 ab	1.69 ± 0.20 b	2.05 ± 0.20 a	1.94 ± 0.11 ab	1.91 ± 0.16 ab
40-50cm	1.67 ± 0.17	1.73 ± 0.09	1.72 ± 0.22	1.98 ± 0.17	1.88 ± 0.12	1.98 ± 0.17

Soil bulk densities showed no significant differences between plots at the depths of 0-10cm, 10-20cm and 40-50cm (table 3). At the depth of 20-30cm, a significant difference exists between plot O and plot S. The same difference is found at 30-40cm but at this depth, P soil bulk density is also significantly higher than S soil bulk density. Appendix B gives a graphical representation of soil bulk density depth evolution at each plot.

3.1.3 Top 50cm SOC stocks

Table 4: SOC stock at study plots and at 5 different depths associated with their standard deviation. Letters indicate the groups determined by a post-hoc tukey pair-wise comparison ("a" class is systematically allocated to the highest value group).

	SOC stock [kgC/m^2]					
depth	P	X	S	O	A	B
0-10cm	1.90 ± 0.08 ab	1.55 ± 0.10 b	1.88 ± 0.10 b	2.00 ± 0.09 ab	2.42 ± 0.25 a	2.07 ± 0.34 a
10-20cm	1.82 ± 0.16 bc	1.71 ± 0.07 c	1.77 ± 0.09 bc	2.09 ± 0.25 bc	2.57 ± 0.27 a	2.18 ± 0.18 ab
20-30cm	2.03 ± 0.48 a	0.99 ± 0.38 b	0.84 ± 0.12 b	2.13 ± 0.15 a	2.28 ± 0.47 a	2.10 ± 0.12 a
30-40cm	0.89 ± 0.11 b	0.46 ± 0.07 b	0.79 ± 0.28 b	1.83 ± 0.31 a	2.04 ± 0.14 a	2.39 ± 0.57 a
40-50cm	0.64 ± 0.06 c	0.54 ± 0.26 c	0.68 ± 0.06 c	1.07 ± 0.09 b	1.94 ± 0.18 a	1.95 ± 0.05 a

By combining the SOCcontent and the bulk density of each sample, a SOC stock can be evaluated for each plot and depth (table 4). SOC stocks follow the same tendencies as found for carbon content. Stocks at plots X and S start decreasing at 20-30cm while at plot P, stock only starts decreasing at 30-40cm. Plots A and B show significantly higher stocks than plots P, X and S at nearly every depth and stay relatively constant through depth. Plot O also contains high SOC stocks but there is a significant difference between O and deposition plots at 10-20cm and 40-50cm. Figure 19 illustrates the decrease in SOC stock following depth at each plot. It shows that the main differences between plots can be found in the amount of C in the lower layers.

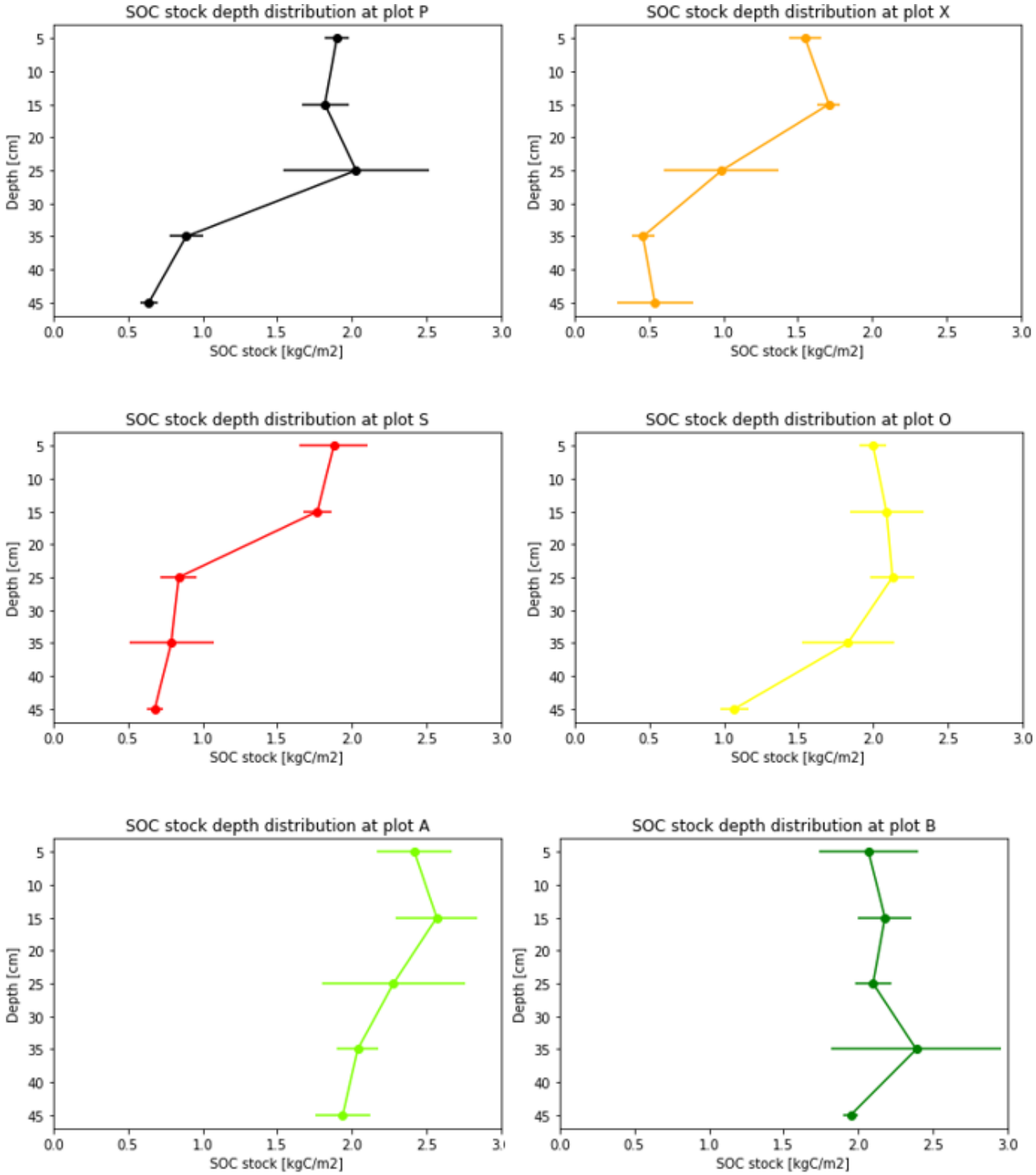

Figure 18: SOC stock depth evolution at each study plot given in table 3. Represented values are the mean SOC stock of the 4 soil cores at a given depth, associated with its standard deviation.

The 50cm topsoil total SOC stocks calculated showed significant differences along the topographic profile (figure 19). Plots where sediment deposition occurs present the highest stocks. Plot A has the most important stock, which is significantly higher than plot O stock, which is itself significantly higher than the stock at control plot P (table 5). C stocks are lower at plots where sediment erosion occurs. Plot X presents a significantly lower stock than plot P.

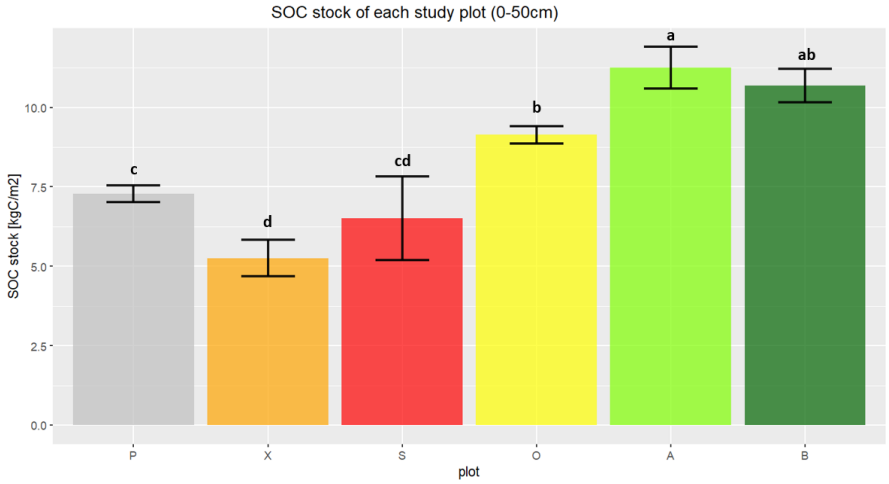

Figure 19: Mean top 50cm SOC stock at each plot associated with the standard deviation. Letters indicate the groups determined by a post-hoc tukey pair-wise comparison ("a" class is systematically allocated to the highest value group).

3.1.4 C/N ratios

As shown in figure 20, the differences observed between topsoil C/N ratios at each study plot are not statistically significant. Measured values range between 9.8 and 13.6, which are values in agreement with recent measurements of C/N ratios in the Belgian loess belt (Krüger et al., 2018).

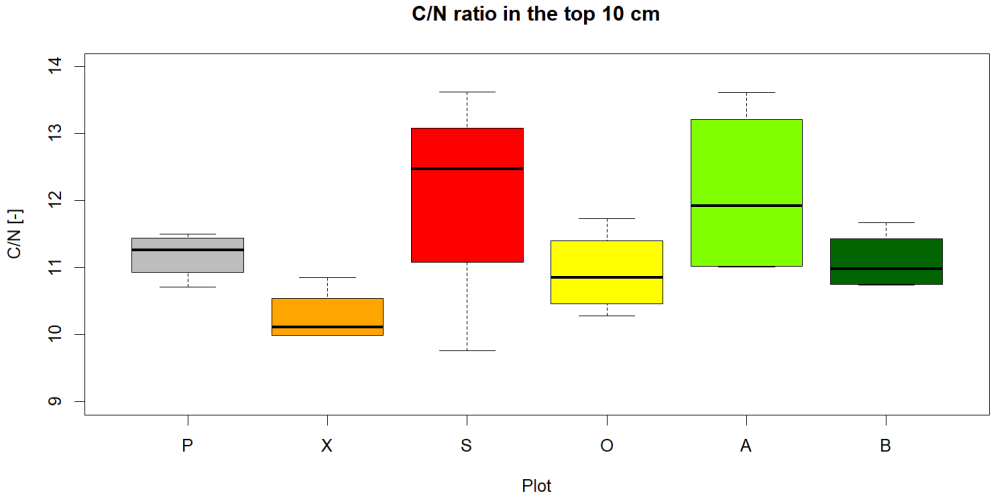

Figure 20: topsoil (0-10cm) C/N ratio at every study plot.

3.1.5 Pedological profiles observation

The observation of soil cores (appendices E, F and G) is in agreement with the data given by the numeric map of Walloon soils. B horizons are clearly identifiable at plot P, X, S and O while plots A and B do not exhibit a clear profile development. Soil cores at deposition plots are dark-coloured from the topsoil to more than 50cm depth, confirming the presence of important SOC stocks at these plots. This also suggests that SOC contents at more than

50cm deep stay high, especially at plot B. Textural wise, texture changes in the deepest part of the soil cores at plot X and plot S suggest proximity to the parent material.

3.2 Soil CO_2 fluxes

3.2.1 Soil respiration through study period

At each plot, the soil CO_2 fluxes were measured 11 times from the 29/3 (day 0) to the 11/7 (day 104) (figure 21). The exact value of the measurements points and their associated standard deviation can be seen in appendix H. The observation of these values already shows some main tendencies. Plots X and S, which represent the erosion scenarios, have higher minimal and maximal mineralisation rates than plots A and B, which represent the deposition scenarios. Moreover, deposition scenarios show less variability than erosion scenarios. While plot A and plot B values lie in the [0.00872 - 0.01563 mgC/gCsoil.hr] and [0.01169 - 0.01737 mgC/gCsoil.hr] intervals, respectively, values of plot X and S lie in the respective ranges of [0.01843 - 0.03867 mgC/gCsoil.hr] and [0.01546 - 0.03461 mgC/gCsoil.hr]. The differences between maximal and minimal values are more than twice larger for erosion plots than for deposition plots.

Values at plot P are similar to values monitored at deposition plots in the first 45 days, while they become similar to those of the erosion plots afterwards. The C flux values at plot O are mostly between the erosion plots and deposition plots values.

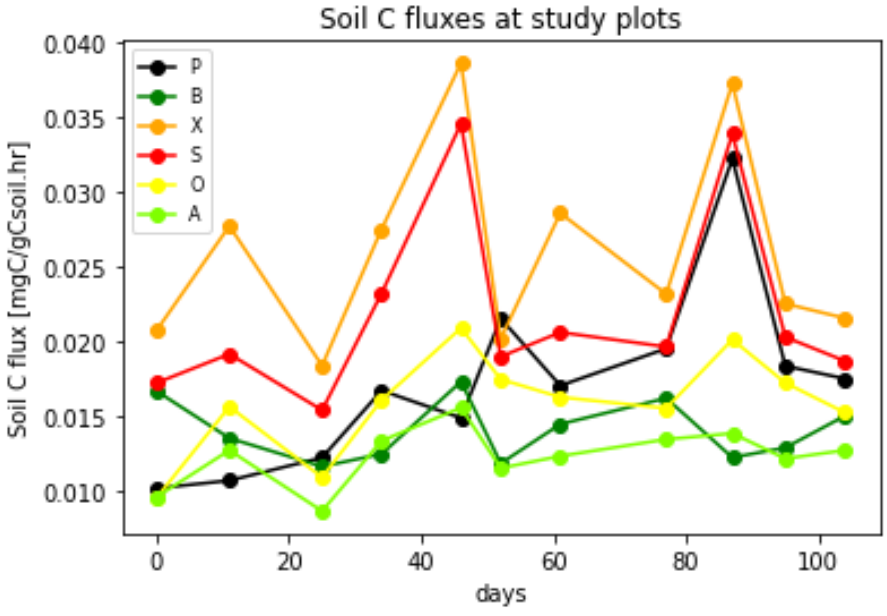

Figure 21: soil C flux rates for each study plot. Measured values are indicated with points on the figure and are the mean values of the 5 measurements at a given plot.

3.2.2 Cumulated mineralisation

As a reminder, cumulated C mineralisation is used as the most direct indicator of SOC global stability in this work. The cumulated C mineralisation (figure 22) values interpolated

from the results shown in section 3.2.1 for the study period confirm the differences between the plots. Erosion plots present the highest cumulated values while deposition plots present the lowest. Plots P and S are situated in between. One can notice that the order of plots going from the highest mineralisation rate to the lowest is exactly the same as the order of plots going from the lowest to the highest SOC stock presented in section 3.1.3.

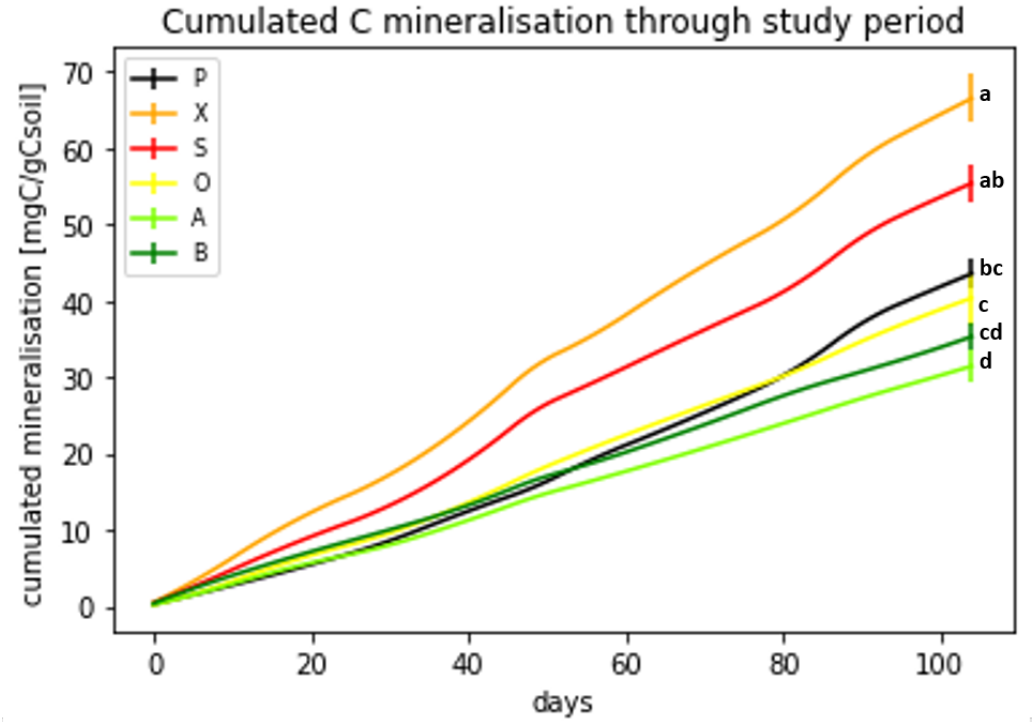

Figure 22: cumulated mineralisation obtained by linearly interpolating C fluxes for days between measurement days. The represented curves are the means of the 5 values of each plot (1 per white collar) and the final value is associated with its standard error. Letters indicate the groups determined by a post-hoc tukey pair-wise comparison.

3.3 Temperature and moisture

Globally, the study period can be separated in three environmental phases (figure 23). The first period, going from day 0 to day 46 is a cold and wet period. The second one (day 47 to day 84) is characterised by higher temperatures but a long period without rain, and thus with decreasing values of soil moisture. The last period (day 85 to day 104) is similar to the second one, with higher temperatures, but an important rain event occurred on day 85 and some smaller rain events occurred from this day and to the end of the study.

Topsoil moisture values range between 0.04 m3/m3 and 0.27 m3/m3. The lowest moistures (between 0.04 and 0.05 m3/m3) were measured on day 77. Topsoil temperature values are situated between 10°C and 26°C. Statistical analyses show no significant difference in the mean temperature (ANOVA) nor in the mean moisture (KRUSKAL-WALLIS) between the six study plots (table 6).

Table 5: mean soil temperature and moisture at each study plot associated with its standard deviation.

Plot	mean temperature [°C]	mean moisture $[m^3/m^3]$
P	16.7 ± 5.3	0.197 ± 0.073
X	19.3 ± 4.2	0.172 ± 0.067
S	17.8 ± 5.5	0.178 ± 0.062
O	16.6 ± 4.2	0.187 ± 0.072
A	17.1 ± 3.8	0.193 ± 0.068
B	17.7 ± 3.8	0.201 ± 0.066

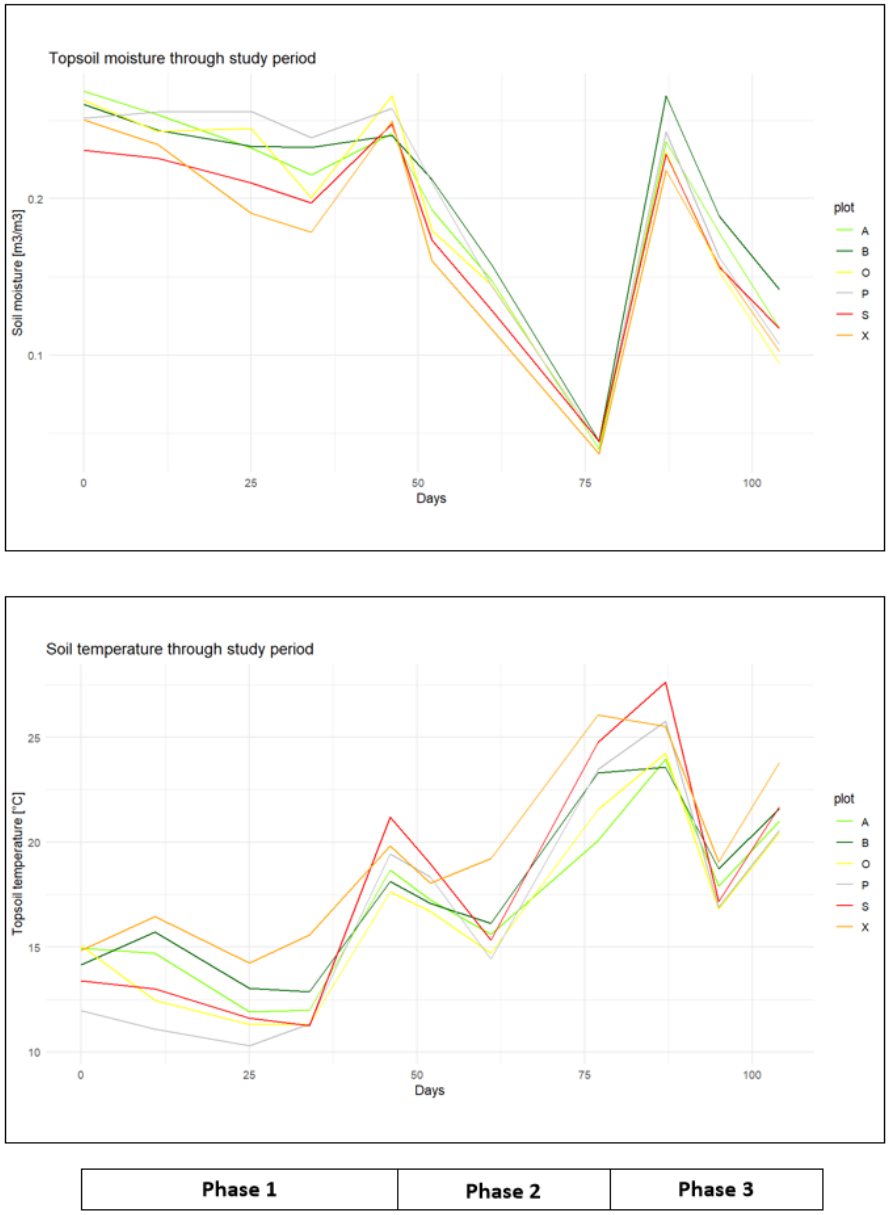

Figure 23: Soil temperature and moisture measurements through study period. Phase 1 corresponds to a wet and cold period, phase 2 and phase 3 are characterised by higher temperature and decreasing soil moisture values.

3.4 Temperature sensivity

Considering that models based on the temperature-soil CO_2 flux relation are developed based only on measurements in conditions without lack of water (Lloyd and Taylor, 1994), the data from day 77, with soil moisture levels around 4%, was not used for model fitting since the wilting point of silty soils is around a 10% moisture[2]. Results show that the Q10 value at plot P is significantly higher than at every other plot. In contrast, plot B is characterised by a significantly lower Q10 value than the 5 other plots. From plot X to plot A, Q10 values follow a decreasing trend but no significant difference is found between the 4 plots. Mean plot Q10 values range between 1.04 and 1.75. In comparison, measured Q10 for croplands in the work of Meyer et al. (2018) range between 1.3 and 2.3.

Figure 24 illustrates well the progressive Q10 diminution from plot P to plot B, with model predictions showing a progressively decreasing slope. RMSE values show no strong differences from a plot to another, especially when observing the RMSE at each plot relatively to the measured mineralisation rates.

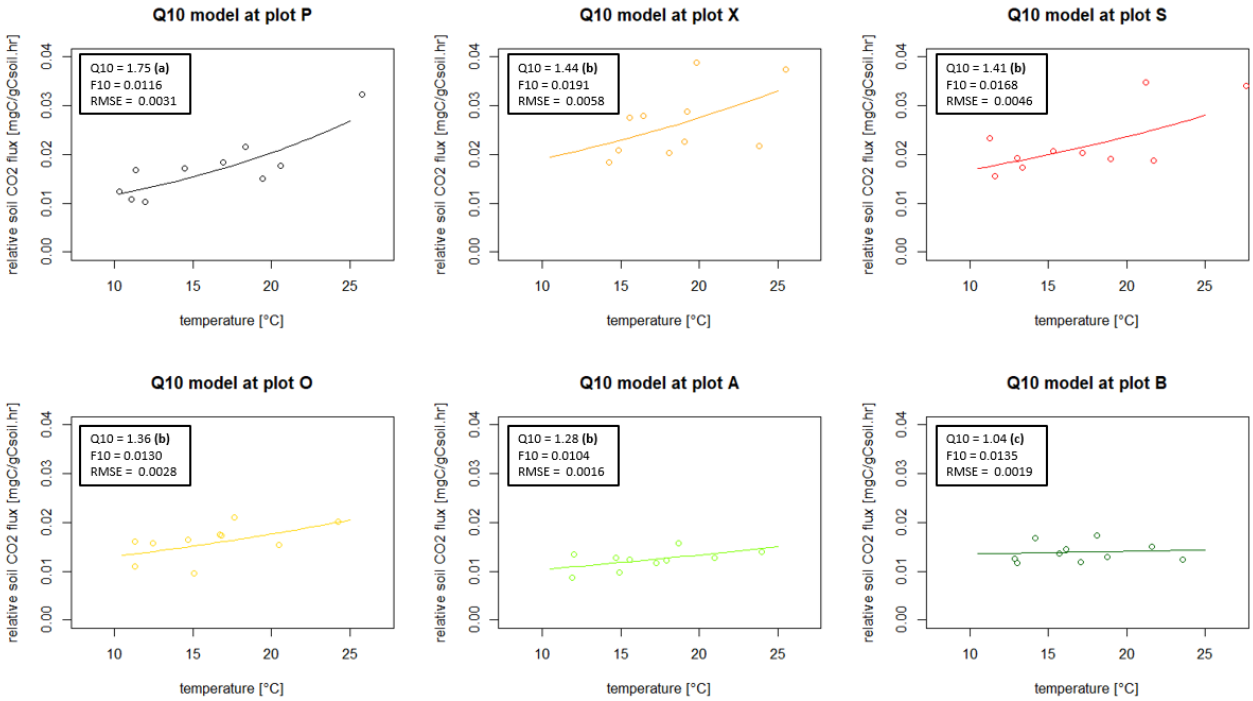

Figure 24: Q10 model predictions (curve) and daily mineralisation rates measured (points) at each plot, associated with model's Q10, F10 and RMSE values.

3.5 C recalcitrance

As detailed in section 2.5, the recovery rate (figure 19) is defined as the ratio between carbon contents measured by dry combustion method (table 2) and by Walkley and Black method (not shown). Although the only significant difference detected by the dunn pair-wise comparison can be found between plot P and plot B, the recovery rate seems to diminish

[2]Portail de l'agriculture wallonne, 10-08-2023

following the topographic profile, going from a mean value of 75.63% at plot P, to 57.67% at plot B. To put it in perspective with literature values, the most common correction factor used to convert Walkley and Black measurements into real SOC contents is 1.33 (Meersmans et al., 2009). This corresponds to a recovery rate value of 75.19%, which agrees with the value measured at plot P. However, other studies measured average recovery rates of 64% in silty loam croplands in north Belgium (Lettens et al., 2007).

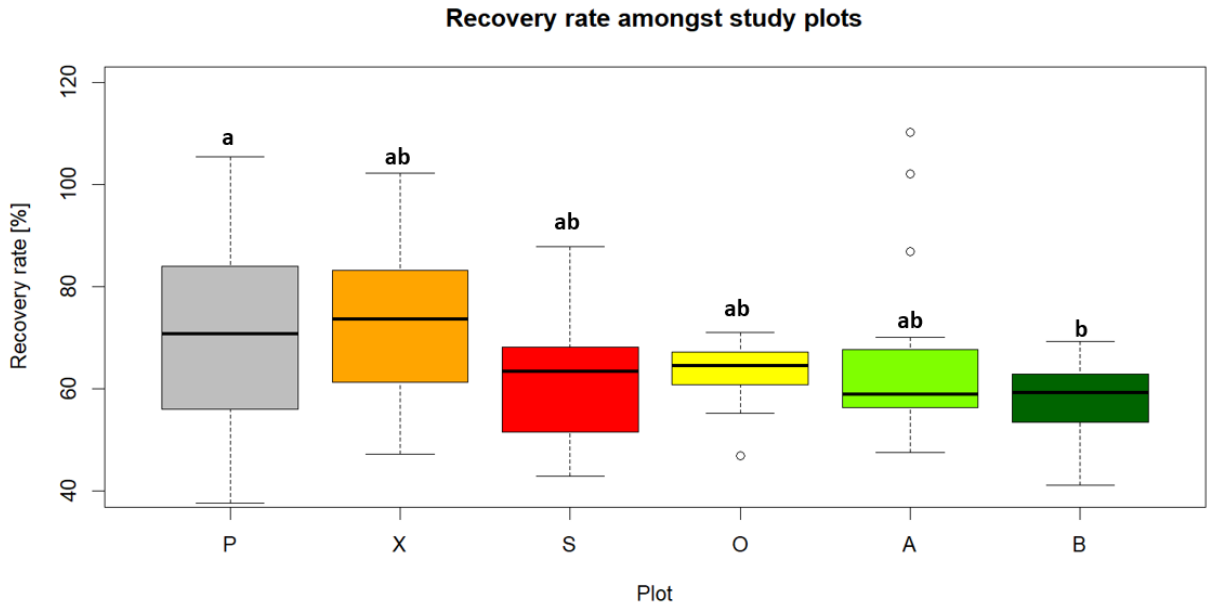

Figure 25: Recovery rates by the Walkley and Black method amongst study plots. Letters indicate the groups determined by a post-hoc dunn pair-wise comparison.

3.6 Soil C fractions

Topsoil fractionation (figure 26) was performed on topsoil samples of 3 plots: plot P which is used as a control plot, plot S where water erosion rate is the highest, and plot B where water deposition rate is the highest. Tillage erosion rates are close to 0 for all of the 3 plots and thus, these results focus only on water erosion effects. Significant differences have been found for the proportion of C contained in the heavy fraction ($< 50\mu m$) between the 3 plots. In plot S, only 20.03% of C is situated in the heavy fraction, while the values for P and B are 36.86% and 48.81%, respectively. Concerning the 50-200µm fraction, significant differences are observed between plot S (11.48%) and the two other plots (24.77% at plot P and 26.58% at plot B). Significant differences exist between the 3 plots regarding their proportion of C found in the 200-2000µm fraction. Plot S has the largest proportion of this fraction (68.49%), followed by plot P (38.49%) and plot B (22.01%). To summarise, plot P is characterised by a balanced repartition of C inside the 3 fractions, plot S is characterised by a larger proportion of fresh C (200-2000µm fraction) and lower proportions of the 2 other fractions and, at last, plot B is characterised by a lower proportion of fresh C and a larger proportion of heavy fraction. Samples from the three other plots are currently undergoing dry combustion analyses at the provincial centre of agriculture and rurality at La Hulpe and results should arrive early-septembre.

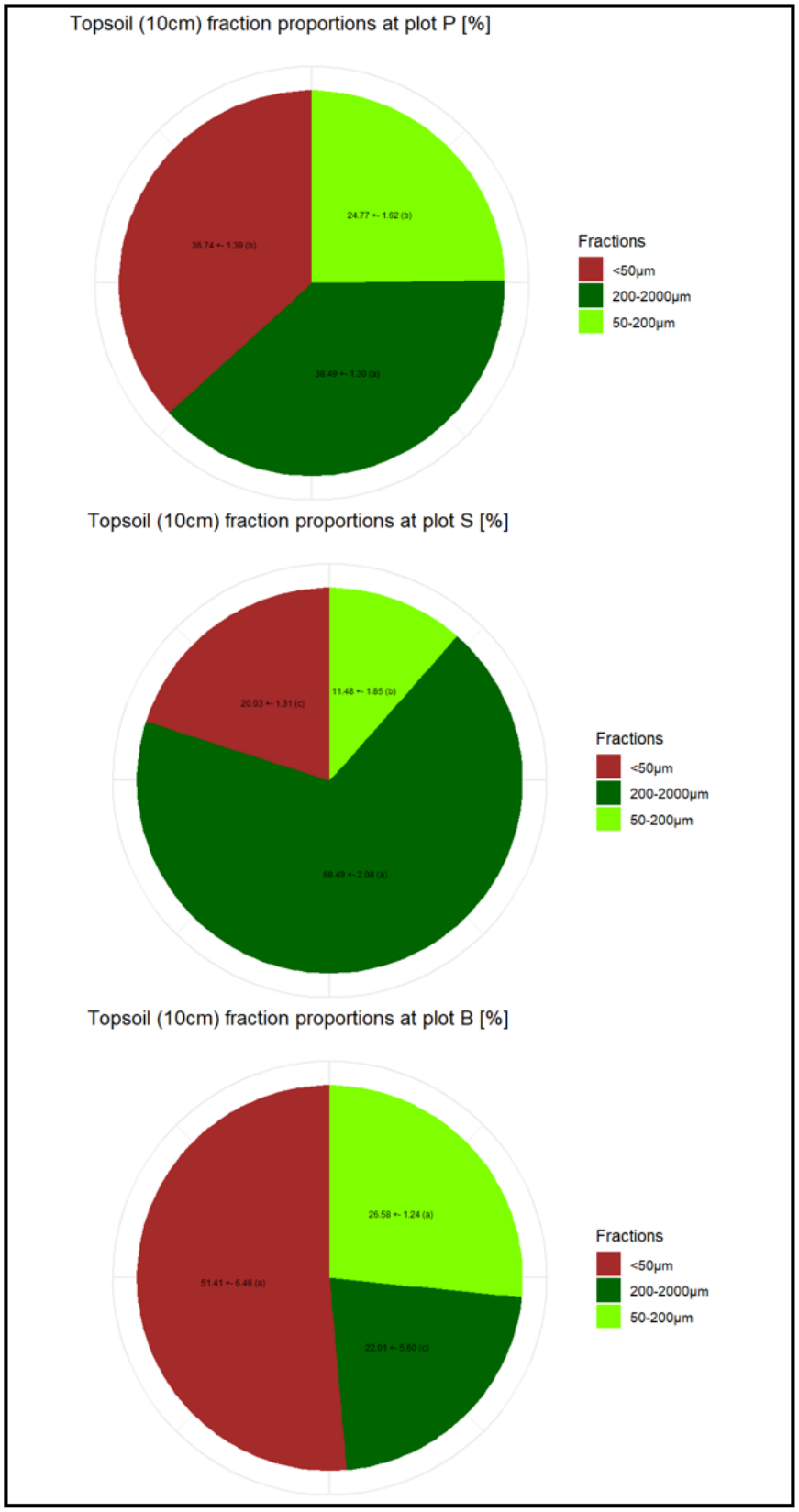

Figure 26: Proportion of the three different C fractions for plots P, S and B. Mean values are indicated and associated with their standard deviation. Letters indicate the groups determined by a post-hoc tukey pair-wise comparison.

4 Discussion

4.1 Effect of erosion on C stability and stabilisation mechanisms

4.1.1 C stability

The first objective of this work was to determine potential impacts of erosion and deposition processes on soil C stability. Results show differences in C stability between the studied scenarios. Two main observations lead to this conclusion.

Firstly, the study of mineralisation rates clearly indicates effects of erosion and deposition processes on C stability. Mineralisation rates are the most direct quantification of C stability because they represent the part of the SOC stock that is lost to the atmosphere due to microbial activity. Plots undergoing erosion present faster mineralisation rates than the control plot undergoing neither erosion nor deposition. Contrarily, plots sustaining deposition processes present slower mineralisation rates (figure 22). This conclusion is in agreement with theoretical patterns established for the same region (Doetterl et al., 2016). The scarcity of field measurements by other studies makes it difficult to compare the quantified values of soil CO_2 fluxes with other data. Most studies use incubation methods and focus on specific parts of the soil such as a particular horizon (Reichstein et al., 2000) or soil pores (Ruamps et al., 2013), without considering the global soil CO_2 flux. It is important to keep in mind that soil respiration values depend on environmental conditions (Maier et al., 2011), with peak activity under hot and moist conditions, as showed by the soil CO_2 flux measurements. Therefore, it can be difficult to compare data from different geographical locations, different parts of the year or different years. However, the amount of soil respiration measurements and the high precision of the SOC content measurements by dry combustion, should guarantee reliable results.

The second observation leading to conclusions on C stability is the fact that erosion and deposition also seem to have an impact on temperature sensitivity of C fluxes. Temperature is assumed to be one of the major factors of soil organisms activity and, thus, on C mineralisation (Lloyd and Taylor, 1994 ; Adjuik and Davis, 2022). Lower temperature sensitivities at deposition plots can be seen through the relatively small variations of measured soil respirations during the study period (figure 21) and lower Q10 values at these plots, especially at plot B (section 3.6). This demonstrates that SOC is well protected from soil organisms at these locations, which means that stabilisation mechanisms are well-developed. The insensitivity to environmental conditions is shown very clearly at the two hot and moist measurements days (days 46 and 87) where soil respiration values from plots X, S and P (only at day 87) peak, while values at plots A and B don't exhibit a clear trend. Lower temperature sensitivities could cause even higher stability differences between deposition locations and other locations in the future with increasing temperatures due to climate change.

4.1.2 Stabilisation mechanisms

After establishing the impact of erosion and deposition processes on global C stability, the second objective of this study was to determine which stabilisation mechanisms these processes directly impact.

The first impact on a stabilisation mechanism identified is the exposure of SOC pools to optimal conditions for activity of soil organisms. While sediment deposition allows large carbon pools to be buried down, sediment erosion exposes C to the surface. This can be observed in the depth distribution of SOC stocks at each plot. (section 3.1.3). It has a major impact on C stability because lower layers present much harsher conditions for microbial activity. Lower layers are more likely to present colder, anoxic and waterlogged conditions than surface layers (Dungait et al., 2012). In the case of deposition locations, the waterlogged conditions in subsoils are even more likely, considering that the surface is closer to the groundwater than at standard or erosion locations. Moreover, subsoils receive low amounts of fresh C inputs, given that these inputs mainly arise from leave or root decomposition. Fresh organic matter represents the most accessible energy form for soil organisms. The low availability in these forms of organic matter makes it difficult for soil organism population to grow, exposing subsoil C to less mineralisation activity (Fontaine et al., 2007). The results of this study have highlighted the major potential for carbon sequestration by subsoils, which has already been mentioned by other studies (Lorenz and Lal, 2005). In contrast, the uplifting of SOC at erosion plots decreases its stability by exposing C to more optimal mineralisation conditions and more fresh C inputs.

The second stabilisation mechanism impacted by erosion processes is the biochemical stability, or recalcitrance, of SOC stocks at each plot. This has been measured through the difference between total C and easily oxidable C at each plot (section 3.3). Based on the values measured during this study, a hypothesis can be made that recalcitrant organic components such as chars are transported from high grounds to the deposition sites. Since erosion preferentially transports labile organic components (Gregorich et al., 1998), one could expect a more progressive gradient of recalcitrant components through the toposequence. This could be the origin of the recovery rate gradient between plot P and plot B. In addition, the observation of much darker topsoils at deposition plots while their topsoil SOC content is only slightly higher than topsoil SOC content at plot P suggests higher char concentrations. However, the Walkley and Black recovery rate of a soil can also be impacted by macroaggregates (Lettens et al., 2007), the formation and resistance of which increase with higher SOC contents (Balesdent, 1996). This could partly explain the lower recovery rates observed at deposition plots, where SOC contents are higher. Yet, aggregates cannot explain the low recovery rates of plots S and O because SOC content at plot S is low and water erosion occurs at both plots, breaking down an important part of the aggregates. Therefore, it is reasonable to assume that the progressive transport of recalcitrant C from high grounds through the slope profile has an impact on recovery rates at the six studied scenarios.

Although it is not necessarily shown by the soil analyses performed in this work, the aggregation breakdown caused by physical alteration at erosion plots and the reaggregation, facilitated by higher SOC contents at deposition plots, have a major impact on carbon stability (Six et al., 2000). These two processes should not be overlooked when analysing the impact of erosion on SOC stability. Aggregates provide high stability for soil C by

physically protecting it from microbial activity. Physical protection can take the form of macroaggregates, microaggregates or microaggregates within macroaggregates (Oades, 1984). Aggregation depends on multiple parameters such as clay content and type (Six et al., 2004).

The impact of erosion on the amount of C contained in the heavy fraction (HF) is more debated. Results show a significant larger proportion of HF at water depositional plot than at control plot, which itself has a significant larger HF proportion than the water erosion plot (section 3.4). At the contrary, plot S contains a high proportion of labile C. This is in contradiction with some studies found in the literature. Indeed, studies indicate that the preferential transport of labile C components by erosion enrich the depositional locations with labile C and diminishes the proportion of labile C on slopes (Gregorich, 1998). This is explained by the fact that the least erosion-resistant macroaggregates are large macroaggregates containing important amounts of labile C (Angers and Giroux, 1996). However, high-intensity rainfalls, which are responsible for 75% of C transport during a cropping season, can carry much more stable C pools (Jacinthe et al., 2004). Usually, heavy rainfalls bring a larger proportion of carried C to surface water but in this study, deposition plots are located just before a layout retaining mud flows. In this situation, heavy rainfalls could play a larger role than usual in C distribution and explain the proportion of HF at deposition locations. In addition to this assumption, the facilitated reaggregation process at depositional plots, could further explain the high proportion of HF found at plot B.

However, this explanation is highly hypothetical and must be verified before taking any conclusion. Another process explaining the high proportion of labile C at erosion locations could be a high rate of dynamic C replacement. Dynamic C replacement occurs when, at eroding locations, the decrease of C content makes it possible for soils to fix fresh C inputs more easily (Harden et al., 1999 ; Kirkels et al., 2014 ; Doetterl et al., 2012). At the contrary, locations with already high SOC contents loose fixing efficiency of fresh C (Feng et al., 2014), explaining the lower proportion of labile C at plot B. The existence of studies both agreeing with and contradicting the results presented in this work shows that the impact of erosion on the fate of labile C remains not fully understood. Although, this study contributes to the idea that dynamic replacement plays a role in SOC dynamics.

All the measured stabilisation mechanisms explain the high C stability at depositional plots. Higher C content in subsoils, higher concentrations in recalcitrant C, enhanced aggregation and higher proportions of HF (here only verified for plot B) all contribute to lower the relative mineralisation rate. The reasons explaining low C stability at erosion plots are not as clear. Erosion plots do not contain less recalcitrant C than plot P and their SOC stocks at 30-40cm and 40-50cm depth are not significantly lower than at plot P. Thus, it seems that aggregate breakdown and subsoil C uplifting are the principal sources of C instability at erosion plots, but this hypothesis should be confirmed with further studies.

Plot O, affected by tillage deposition and water erosion, has a particular configuration. Its stability lies between stability at the control plot and stability at depositional plots. An indicator of this in-between situation is the soil respiration values at the two hot and moist days (days 46 and 87), where values present peaks, but smaller than those at plot X and S. The C characteristics observed at plot O also show this in-between behaviour. Subsoil SOC stocks lie between stocks at P and stocks at deposition plots. The amount of recalcitrant C is also in between those observed at plot P and at deposition plots. Tillage deposition contributes

to the burial of SOC stocks and water erosion is responsible for aggregate breakdown. The stabilisation of buried C by tillage deposition and the fact that the intensity of water erosion is limited at plot O explain why mineralisation rate at plot O is situated between the values found at plot P and at deposition plots. Moreover, the high SOC content at plot O inhibits the dynamic C replacement and, thus, should limit the proportion of labile C, characterised by a higher mineralisation rate, at this location. However, the last assumption should be supported by further measurements.

4.1.3 Specific attention on tillage erosion impact

Most studies only focus on water erosion-induced C distribution. Recently, the impact of other erosion modalities such as tillage erosion is being addressed and estimations predict that tillage erosion rates exceed water erosion rates in numerous geographical locations (Van Oost et al., 2005). Such soil redistribution goes along with C redistribution and potential impacts on C stability at eroded convexities and at concavities where sediments are deposited (Heckrath et al., 2005). This study is in complete agreement with the last affirmation. The results highlight the impact of tillage erosion on SOC distribution, with plot X and plot A being the plots with the smallest and the greatest 50cm SOC stock, respectively. The impact on C stability is also highlighted by the mineralisation rates at these plots, which are also the lowest and the highest amongst the study field.

However, impacts on C stabilisation mechanisms remain more unknown. As mentioned previously, the impact of tillage erosion on C stability at study plots can be explained by the transport of SOC from convexities to concavities, causing SOC burial at deposition locations and the accumulation of labile C with high mineralisation rates at erosion locations (Van Oost et al., 2005). Measurements of recalcitrant C distribution and environmental conditions did not lead to additional observations that could explain such stability differences. Thus, it is hard to understand why locations affected by tillage erosion or deposition have the most extreme mineralisation rate values. An explanation could reside in the fact that plot X undergoes light water erosion in addition to tillage erosion and plot A undergoes light water deposition in addition to tillage deposition. This study demonstrates the impact of tillage erosion on C stocks distribution and C stability but, identifying impacts on other stabilisation mechanisms require further studies. This difficulty is emphasized by the very small number of studies investigating all stabilisation mechanisms at play.

4.2 Erosion: C source or sink?

The last study objective was to contribute as much as possible to the debate establishing if the global impact of erosion on soil carbon sequestration is positive or negative. Pierre Baert already contributed to this debate by observing SOC stocks in the first 1m of soil at plateaus, slopes and bottom slopes on the same field during his master thesis in 2022. His conclusion went from a slight sink impact when looking to SOC stock model predictions to a slight source impact when looking to his measurements, highlighting the difficulty to answer this question. The present study therefore tries to respond with another complementary approach, by investigating the impact of erosion on soil C dynamics and stability rather than on stocks.

The negative effects of erosion on C stability identified during this study mainly stem from the destruction of aggregates and the uplifting of SOC at erosion plots. This process

occurs at locations with the smallest SOC stocks. On the other hand, more numerous positive effects of erosion are identified. A large amount of C is buried on deposition locations, placing it in conditions less favourable to the activity of soil organisms and allowing re-aggregation. This leads to a stabilisation of SOC stocks where erosion processes concentrate C. Moreover, the decrease of SOC contents at erosion plots allows a dynamic C replacement, fixing fresh inputs that could not have been fixed otherwise. The fixing of fresh labile C at erosion locations has a negative impact on mean mineralisation rates at erosion plots while it has a positive impact on total soil C sequestration. The exact mass of C sequestered by dynamic replacement still needs to be quantified more precisely.

In a first instance, erosion seems to have a positive impact on C sequestration, with more positive effects than negative effects and with the positive effects acting where the largest SOC stocks can be found. However, a first important parameter in the calculation of a global impact is the ratio between erosion locations surface and deposition locations surface. It is important to estimate the proportion of the total SOC stock of croplands being stabilised by deposition processes and the proportion of SOC being disrupted by erosion processes. In addition, numerous negative impacts of erosion on SOC stocks are not addressed in this study, as detailed below.

Firstly, all eroded sediments do not necessarily deposit on downslope locations. Studies estimate that around 20% of the sediments put in motion by water erosion reach the ocean (Stallard, 1998). This is a large part of sediments that probably also contain an important amount of SOC. It is difficult to quantify the SOC loss, but it certainly represents a non-negligible impact of erosion on SOC stocks. However, this affirmation does not concern tillage erosion.

Secondly, erosion is a major soil degradation process and has a significant impact on the crop productivity by affecting soil properties and nutrient distribution. This is true for both tillage erosion (Van Oost et al., 2006) and water erosion (Lal and Moldenhauer, 1987). The decrease of crop production goes along with a decrease of C inputs into soils, since plant residues and dead roots are one of the principal C inputs in cropland soils (Kuzyakov and Domanski, 2000 ; Dynarski et al., 2020). Once again, it is difficult to precisely quantify the impacts of fertility decrease on soil C sequestration.

Moreover, another C loss caused by erosion that has not been calculated in this study is the mineralisation during transport. Indeed, SOC undergoes destabilisation processes while it is transported, which causes C mineralisation (de Nijs and Cammeraat, 2020). The measured amount of mineralised C during transport varies between studies but, in the Belgian loess belt, it has been estimated that less than 10% of transported C is mineralised in the weeks following a heavy erosion event (Van Hemelryck et al., 2011). Thus, this amount must be added to the SOC losses caused by erosion events. The proportion of mineralised C during the transport phase of less intense erosion events remains unknown. The mechanisms governing such losses also remain poorly understood (de Nijs and Cammeraat, 2020).

Finally, the concentration of high SOC quantities at some locations could make them reach their maximum potential of C content, and thus, limit the benefits of erosion on C stability in the long term. Indeed, soils have a maximal content of C in the stable fraction, which depends on soil physical and chemical characteristics as well as land use (Barré et al., 2017). Continuously adding C to deposition soils could in the long term prevent them to

be able to stabilise new C inputs (Feng et al., 2013). Soil C stabilisation efficiency could even decrease with the soil progressively saturating in SOC (Feng et al., 2014). Therefore, concentrating C at certain locations instead of distributing the SOC stocks homogeneously could represent an unsustainable strategy.

4.3 Effects on SOC stock distribution

Beyond the effects of erosion processes on C stability that are mentioned above, the results also confirmed the impact of erosion processes on SOC stocks distribution. Erosion results in a horizontal and in a vertical movement of organic C, as showed by numerous studies (Van Oost et al., 2005). SOC stocks measurements at the different plots indicate that the most significant differences between plots can be found in the lowest part of the soil cores, highlighting the intensity of vertical transport of C by erosion.

Overall, tillage erosion seems to have more impact on SOC distribution than water erosion since plot X and plot A have the smallest and the largest top 50cm stock, respectively. This could however vary from a field to another, but it indicates once again the importance of establishing a better understanding of tillage erosion mechanisms, that have received less attention than water and wind erosion mechanisms (Van Oost et al., 2006).

Thus, considering the impact of both tillage and water erosion on SOC distribution and on SOC stability, SOC stocks models should account for erosion (Meersmans et al., 2008). Initiatives for incorporating erosion components in SOC stock models at relatively low resolution ($1km^2$) have already been undertaken (Lugato et al., 2016). However, as explained in the previous section, the larger the scale considered, the larger the uncertainties on the net effects of erosion on SOC stocks. With the recent interest in establishing higher resolution stocks models (Meersmans et al., 2011), the necessity of taking erosion processes into account should rise. Indeed, at the scale of the study field, results showed that erosion can induce up to twofold variations in SOC stock between plot X and A, for example. This could improve model accuracy, especially for small-scale models, but also for erosion models predicting erosion rates for watersheds based on the RUSLE equation, where carbon content influences the calculated soil loss rates via the soil erodibility factor K (Ghosal and Das Bhattacharya, 2020).

Results on recovery rates of the Walkley and Black method could also have implications for SOC stock models since they show that the difference between the Walkley and Black method measurements and the dry combustion measurements grows along the toposequence. Indeed, these measurements are often used for large sampling campaigns because of its low-cost and simple character, and ultimately, for spatial SOC stock models (Meersmans et al., 2009). Generally, a coefficient factor of 1.33 is used to convert Walkley and Black measurements into real SOC contents. Using different values of coefficient factors depending on topographic situations could be an option to increase model precision. This type of solution has already been proposed to improve C quantification by Walkley and Black for different land uses (Brye and Slaton, 2003).

4.4 Limitations of the study

4.4.1 Sampling design

The sampling design of this study implies some uncertainties. Firstly, the fact that each scenario has only been attributed one plot could explain potential differences with other studies. Although it would heavily increase the number of required measurements, increasing the number of plots per erosion scenario could bring more certitude to the observed tendencies. This is especially true for plots where the two erosion processes are at play. For example, the value of water erosion rates at plot X and plot O could have an impact on the mineralisation rates and stabilisation mechanisms, and different plots following the same theoretical scenario could therefore present different mineralisation rates. Erosion and deposition rates have been calculated in the master thesis of Pierre Baert (2022), but the model errors and the relatively low resolution of predictions (one value per 20x20m square) doesn't allow the precision needed. Therefore, it could be relevant to measure erosion rates of each plot with higher resolution soil erodibility estimations.

Also, it should be relevant to study the effects on a higher scale, such as a watershed. Indeed, stability differences could potentially be even larger within a watershed than within a singular field. The time scale of the study could also be enlarged to a whole year, including winter and fall, or several years if possible. This would allow to observe stability differences through a maximal number of environmental conditions. Upscaling the study could potentially lead to new conclusions but it is difficult to accomplish field measurements on large periods, especially on croplands where machinery has to intervene multiple times a year.

Moreover, the SOC stock analysis and the visual observation of soil cores of 80cm depth suggest that non-negligible stocks of C are situated below 50cm. This results in the underestimation of global C stability, especially at plots A and B and, to a lesser extent, at plot O. The results confirm that a lot of previous works, focussing on topsoil alone, could have led to incomplete or partially inaccurate conclusions (Doetterl et al., 2016). Overall, it seems now clear that studying global SOC stability must go along with precise understanding of subsoil SOC stocks. Increasing the sample depth and carrying out SOC measurements and quantifying stabilisation mechanisms at each depth looks therefore an important addition to the measurements already realised.

4.4.2 Detangling root respiration from soil respiration

Root respiration, while being a major component of soil respiration, has not been addressed in this work. Indeed, measured soil $CO2$ fluxes are the combination of heterotrophic respiration by soil organisms and autotrophic respiration by plant roots. For croplands sown with wheat, root respiration accounts for at least 75% of the measured fluxes (Hanson et al., 1999). Even though the removal of plants in the white collar two weeks before and during the study period should limit the part of root respiration in the total $CO2$ flux, it is likely that root respiration still is an important part of the measured mineralisation rates. This is confirmed by the observation of the root network (figure 12) under the white collars at the end of the study period.

A wide variety of methods are available to estimate the part of root respiration in soil fluxes (Hanson et al., 1999). The most precise, but complex, methods are the isotopic methods based on isotopic differences between C emitted by roots or microorganisms. Such methods can estimate the part of root respiration at specific moments and make it possible to establish the evolution of this part through the study period. Exact SOC mineralisation rates can then be calculated.

More simple and affordable methods, called root exclusion methods, have the capacity to greatly limit the part of root respiration in soil fluxes. One of these methods could have been applied to this study. This method, called "trenching", consists in cutting plants above ground, which has been done during this study, in addition to digging trenches around the plot to cut the roots, and placing physical barriers avoiding root development from plants outside the plot. Subsequent measurements of soil fluxes on the plot only depend on soil C mineralisation. This method has two major drawbacks (Hanson et al., 1999). Firstly, the plot needs to be set up multiple months before the beginning of the study to avoid the impact of fast-decomposing dead roots. This makes it difficult to implement on field studies for cultivated cropland where machinery must operate. Secondly, trenching can have an impact on soil properties such as moisture or temperature and, therefore, on mineralisation rates.

Even though root respiration represents an important part of the measured soil mineralisation rates, it should not drastically change the conclusions on stability differences between plots. Indeed, cultural practices are identic all along the study field and the amount of root respiration is likely to be similar amongst the six plots. The fact that the study field grows three different varieties of wheat could however be responsible of some slight differences. Nevertheless, the neglect of root respiration must be considered when comparing measured mineralisation rates with other studies.

4.4.3 Unstudied stability factors

It is necessary to keep in mind that the studied stabilisation mechanisms are far from being the only ones regulating C stability. Mechanisms such as physical protection (Six et al., 2002) have not been directly measured during this study. It would be interesting to understand in which physical conditions soil C is distributed at each plot: in macroaggregates, in microaggregates, bound with fine particles or free. Though, measuring those precise characteristics require more complex and time demanding protocols such as the one presented by Tan et al. (2007). Applying a more complex soil fractionation protocol could clearly identify the part of C situated inside aggregates and the part of C chemically bonded with the fine fraction. It would bring precious complementary information on the effects of erosion on those two major stabilisations mechanisms. This is especially true since the hypothesis of aggregation breakdown at erosion locations and reaggregation at deposition locations is suspected to play a major role in C stability.

Biochemical stabilisation has only been partly considered by the comparison between Walkley and Black and dry combustion methods, allowing to quantify the part of hardly oxidable C. However, other parameters can be measured, such as hydrolysability by water or acids. Those extractions simulate the type of chemical attacks that soil C can undergo and are linked with C recalcitrance (von Lützow et al., 2007). Physical and biochemical analyses could bring additional information on the influence of erosion on SOC stability.

Besides, numerous erosion impacts must be clarified. Dynamic replacement of organic C at erosion plots could potentially play a major role in soil C sink abilities and this process must be furthered. Other parameters such as transport mineralisation, maximal soil C contents, fertility losses must be quantified more precisely. Currently, the lack of quantification is one of the main obstacles to establishing the sink or source outcome of soil erosion.

4.5 Perspectives

The numerous conclusions drawn from this work call this study to be extended in a more general context. Therefore, upscaling the available data could bring valuable information and allow to generalise the understanding of erosion on C stability and stabilisation mechanisms. This upscaling can be done in time, by effecting measurements during the second part of the summer, and during the colder period of the year. These periods have been investigated for logistical reasons and would bring some observations of mineralisation rates under other environmental conditions. The study could also be upscaled in terms of study field properties such as soil texture, agricultural practices, and crop cover since they could have an impact on the effects of erosion on soil C.

This study provides an approximation of the stability of SOC stocks on the field, making it possible to assess the source or sink potential of erosion processes. However, this is only one of the components of the total carbon balance of erosion. Other components are the SOC losses to surface water, SOC losses during sediment transport, dynamic C replacement, and the decrease of C inputs due to fertility decrease. Those four components could be estimated by specific studies. Put together, a more complete quantification of the sink or source potential could be established. Such a comprehensive view of the stability of SOC stocks is important in the framework of soil carbon sequestration policy making.

5 Conclusions

The aim of this study was to assess the effect of water and tillage erosion on soil C dynamics in a silty soil in central Belgium, in order to determine the global impact of erosion processes on SOC stocks. Therefore, both global stability and stabilisation mechanisms were measured through numerous parameters. Global stability is clearly impacted by erosion, with deposition locations having low C mineralisation rates and low temperature sensitivities of soil CO_2 fluxes. At the contrary, mineralisation rates at erosion locations are significantly higher than at the rest of the study field. Low stability locations are characterised by low SOC stocks while high stability locations present the highest SOC stocks.

These stability differences among the plots can be ascribed to different intensities in C stabilisation mechanisms. Measurements suggest that water erosion generates a progressive concentration gradient of the most biochemically recalcitrant forms of C along the slope, with the highest values at the bottom slopes. Although soil C fractionation could only be applied to plots affected by water erosion, bottom slope plot showed a higher proportion of chemically bound C to silt and clay particles than control plot. At the contrary, the eroded plot has a lower proportion of bound C and a high proportion of young labile C, suggesting an impact of dynamic C replacement on soil C sequestration. Measurements highlight the effects of erosion processes on SOC distribution and SOC stability, and thus, on soil C dynamics. However, since other impacts of erosion on C losses cannot be quantified with the measurements nor the literature, further studies are required to draw definite conclusions about the global effect of tillage and water erosion on C stocks.

6 Contribution

This master thesis implicated numerous field work and manipulations. The student achieved:

1. Soil sampling on field with the help of Jeroen Meersmans and Nicolas Kovacs
2. Soil ample drying, crushing and sieving
3. Soil bulk density calculations
4. Carbon quantification following the Walkley and Black method
5. Soil fractionation
6. All soil respiration measurements on field
7. All soil temperature and moisture measurements on field

References

Adjuik, T. A., & Davis, S. C. (2022). Machine learning approach to simulate soil CO2 fluxes under cropping systems. *Agronomy*, *12*(1), 197. https://doi.org/10.3390/agronomy12010197

Angers, D. A., & Giroux, M. (1996). Recently deposited organic matter in soil water-stable aggregates. *Soil Science Society of America Journal*, *60*(5), 1547–1551. https://doi.org/10.2136/sssaj1996.03615995006000050037x

Balesdent, J. (1991). Effets des ultrasons sur la distribution granulométrique des matières organiques des sols.

Balesdent, J. (1996). Un point sur l'évolution des réserves organiques des sols en France. *Étude et Gestion des Sols*.

Barré, P., Angers, D. A., Basile-Doelsch, I., Bispo, A., Cécillon, L., Chenu, C., Chevallier, T., Derrien, D., Eglin, T. K., & Pellerin, S. (2017, September 22). *Ideas and perspectives: Can we use the soil carbon saturation deficit to quantitatively assess the soil carbon storage potential, or should we explore other strategies?* (preprint). Biogeochemistry: Soils. https://doi.org/10.5194/bg-2017-395

Beule, L., Vaupel, A., & Moran-Rodas, V. E. (2022). Abundance, diversity, and function of soil microorganisms in temperate alley-cropping agroforestry systems: A review. *Microorganisms*, *10*(3), 616. https://doi.org/10.3390/microorganisms10030616

Bielders, C., Ramelot, C., & Persoons, E. (2003). Farmer perception of runoff and erosion and extent of flooding in the silt-loam belt of the belgian walloon region. *Environmental Science & Policy*, *6*(1), 85–93. https://doi.org/10.1016/S1462-9011(02)00117-X

Bollinne, A., & Pissart, A. (1978). Erosion des sols limoneux cultivés de Hesbaye.

Bollinne, A., & Rosseau, P. (1978). L'érodibilité des sols de moyenne et haute belgique: Utilisation d'une méthode de calcul du facteur k de l'équation universelle de perte de sol. *Bulletin de la société géographique de Liège*.

Brodowski, S., John, B., Flessa, H., & Amelung, W. (2006). Aggregate-occluded black carbon in soil: Occluded black carbon in soil. *European Journal of Soil Science*, *57*(4), 539–546. https://doi.org/10.1111/j.1365-2389.2006.00807.x

Brye, K. R., & Slaton, N. A. (2003). Carbon and nitrogen storage in a typic albaqualf as affected by assessment method. *Communications in Soil Science and Plant Analysis*, *34*(11), 1637–1655. https://doi.org/10.1081/CSS-120021302

Conen, F., Zimmermann, M., Leifeld, J., Seth, B., & Alewell, C. (2008). Relative stability of soil carbon revealed by shifts in 15n and c:n ratio.

Conyers, M. K., Poile, G. J., Oates, A. A., Waters, D., & Chan, K. Y. (2011). Comparison of three carbon determination methods on naturally occurring substrates and the implication for the quantification of 'soil carbon'. *Soil Research*, *49*(1), 27. https://doi.org/10.1071/SR10103

De Vos, B., Lettens, S., Muys, B., & Deckers, J. A. (2007). Walkley?black analysis of forest soil organic carbon: Recovery, limitations and uncertainty. *Soil Use and Management*, *23*(3), 221–229. https://doi.org/10.1111/j.1475-2743.2007.00084.x

de Nijs, E. A., & Cammeraat, E. L. (2020). The stability and fate of soil organic carbon during the transport phase of soil erosion. *Earth-Science Reviews*, *201*, 103067. https://doi.org/10.1016/j.earscirev.2019.103067

Doetterl, S., Cornelis, J.-T., Six, J., Bodé, S., Opfergelt, S., Boeckx, P., & Van Oost, K. (2015). Soil redistribution and weathering controlling the fate of geochemical and physical car-

bon stabilization mechanisms in soils of an eroding landscape. *Biogeosciences*, *12*(5), 1357–1371. https://doi.org/10.5194/bg-12-1357-2015

Doetterl, S., Berhe, A. A., Nadeu, E., Wang, Z., Sommer, M., & Fiener, P. (2016). Erosion, deposition and soil carbon: A review of process-level controls, experimental tools and models to address c cycling in dynamic landscapes. *Earth-Science Reviews*, *154*, 102–122. https://doi.org/10.1016/j.earscirev.2015.12.005

Doetterl, S., Six, J., Van Wesemael, B., & Van Oost, K. (2012). Carbon cycling in eroding landscapes: Geomorphic controls on soil organic c pool composition and c stabilization. *Global Change Biology*, *18*(7), 2218–2232. https://doi.org/10.1111/j.1365-2486.2012.02680.x

Dungait, J. A. J., Hopkins, D. W., Gregory, A. S., & Whitmore, A. P. (2012). Soil organic matter turnover is governed by accessibility not recalcitrance. *Global Change Biology*, *18*(6), 1781–1796. https://doi.org/10.1111/j.1365-2486.2012.02665.x

Dynarski, K. A., Bossio, D. A., & Scow, K. M. (2020). Dynamic stability of soil carbon: Reassessing the "permanence" of soil carbon sequestration. *Frontiers in Environmental Science*, *8*, 514701. https://doi.org/10.3389/fenvs.2020.514701

Feller, C. (1994). La matière organique dans les sols tropicaux à argile 1:1 : recherche de compartiments organiques fonctionnels : une approche granulométrique.

Feng, W., Plante, A. F., Aufdenkampe, A. K., & Six, J. (2014). Soil organic matter stability in organo-mineral complexes as a function of increasing c loading. *Soil Biology and Biochemistry*, *69*, 398–405. https://doi.org/10.1016/j.soilbio.2013.11.024

Feng, W., Plante, A. F., & Six, J. (2013). Improving estimates of maximal organic carbon stabilization by fine soil particles. *Biogeochemistry*, *112*(1), 81–93. https://doi.org/10.1007/s10533-011-9679-7

Fontaine, S., Barot, S., Barré, P., Bdioui, N., Mary, B., & Rumpel, C. (2007). Stability of organic carbon in deep soil layers controlled by fresh carbon supply. *Nature*, *450*(7167), 277–280. https://doi.org/10.1038/nature06275

Frank, S., Schmid, E., Havlík, P., Schneider, U. A., Böttcher, H., Balkovič, J., & Obersteiner, M. (2015). The dynamic soil organic carbon mitigation potential of european cropland. *Global Environmental Change*, *35*, 269–278. https://doi.org/10.1016/j.gloenvcha.2015.08.004

Gavinelli, E., Feller, C., Larré-Larrouy, M., Bacye, B., Djegui, N., & Nzila, J. d. D. (1995). A routine method to study soil organic matter by particle-size fractionation: Examples for tropical soils. *Communications in Soil Science and Plant Analysis*, *26*(11), 1749–1760. https://doi.org/10.1080/00103629509369406

Gerke, J. (2022). The central role of soil organic matter in soil fertility and carbon storage. *Soil Systems*, *6*(2), 33. https://doi.org/10.3390/soilsystems6020033

Ghosal, K., & Das Bhattacharya, S. (2020). A review of RUSLE model. *Journal of the Indian Society of Remote Sensing*, *48*(4), 689–707. https://doi.org/10.1007/s12524-019-01097-0

Glenk, K., & Colombo, S. (2011). Designing policies to mitigate the agricultural contribution to climate change: An assessment of soil based carbon sequestration and its ancillary effects. *Climatic Change*, *105*(1), 43–66. https://doi.org/10.1007/s10584-010-9885-7

Gregorich, E., Greer, K., Anderson, D., & Liang, B. (1998). Carbon distribution and losses: Erosion and deposition effects. *Soil and Tillage Research*, *47*(3), 291–302. https://doi.org/10.1016/S0167-1987(98)00117-2

Hakoun, V., Orban, P., Dassargues, A., & Brouyère, S. (2017). Factors controlling spatial and temporal patterns of multiple pesticide compounds in groundwater (hesbaye chalk

aquifer, belgium). *Environmental Pollution*, *223*, 185–199. https://doi.org/10.1016/j.envpol.2017.01.012

Hanson, P. J., Edwards, N. T., Garten, C. T., & Andrews, J. A. (1999). Separating root and soil microbial contributions to soil respiration: A review of methods and observations.

Harden, J. W., Sharpe, J. M., Parton, W. J., Ojima, D. S., Fries, T. L., Huntington, T. G., & Dabney, S. M. (1999). Dynamic replacement and loss of soil carbon on eroding cropland. *Global Biogeochemical Cycles*, *13*(4), 885–901. https://doi.org/10.1029/1999GB900061

Heckrath, G., Djurhuus, J., Quine, T. A., Oost, K. V., Govers, G., & Zhang, Y. (2005). Tillage erosion and its effect on soil properties and crop yield in denmark. *J. ENVIRON. QUAL.*, *34*.

Jacinthe, P.-A., Lal, R., Owens, L., & Hothem, D. (2004). Transport of labile carbon in runoff as affected by land use and rainfall characteristics. *Soil and Tillage Research*, *77*(2), 111–123. https://doi.org/10.1016/j.still.2003.11.004

Kirkels, F., Cammeraat, L., & Kuhn, N. (2014). The fate of soil organic carbon upon erosion, transport and deposition in agricultural landscapes — a review of different concepts. *Geomorphology*, *226*, 94–105. https://doi.org/10.1016/j.geomorph.2014.07.023

Kleber, M. (2010). What is recalcitrant soil organic matter? *Environmental Chemistry*, *7*(4), 320. https://doi.org/10.1071/EN10006

Knicker, H. (2007). How does fire affect the nature and stability of soil organic nitrogen and carbon? a review. *Biogeochemistry*, *85*(1), 91–118. https://doi.org/10.1007/s10533-007-9104-4

Kouli, M., Soupios, P., & Vallianatos, F. (2009). Soil erosion prediction using the revised universal soil loss equation (RUSLE) in a GIS framework, chania, northwestern crete, greece. *Environmental Geology*, *57*(3), 483–497. https://doi.org/10.1007/s00254-008-1318-9

Krüger, I., Chartin, C., van Wesemael, B., & Carnol, M. (2018). Defining a reference system for biological indicators of agricultural soil quality in wallonia, belgium. *Ecological Indicators*, *95*, 568–578. https://doi.org/10.1016/j.ecolind.2018.08.010

Krull, E. S., Baldock, J. A., & Skjemstad, J. O. (2003). Importance of mechanisms and processes of the stabilisation of soil organic matter for modelling carbon turnover. *Functional Plant Biology*, *30*(2), 207. https://doi.org/10.1071/FP02085

Kuhn, N. J. (2007). Erodibility of soil and organic matter: Independence of organic matter resistance to interrill erosion. *Earth Surface Processes and Landforms*, *32*(5), 794–802. https://doi.org/10.1002/esp.1486

Kuzyakov, Y., & Domanski, G. (2000). Carbon input by plants into the soil. review. *Journal of Plant Nutrition and Soil Science*, *163*(4), 421–431. https://doi.org/10.1002/1522-2624(200008)163:4<421::AID-JPLN421>3.0.CO;2-R

Lal, R. (2013). Soil carbon management and climate change. *Carbon Management*, *4*(4), 439–462. https://doi.org/10.4155/cmt.13.31

Lal, R., & Moldenhauer, W. C. (1987). Effects of soil erosion on crop productivity. *Critical Reviews in Plant Sciences*, *5*(4), 303–367. https://doi.org/10.1080/07352688709382244

Lettens, S., De Vos, B., Quataert, P., van Wesemael, B., Muys, B., & van Orshoven, J. (2007). Variable carbon recovery of walkley-black analysis and implications for national soil organic carbon accounting. *European Journal of Soil Science*, *58*(6), 1244–1253. https://doi.org/10.1111/j.1365-2389.2007.00916.x

Lloyd, J., & Taylor, J. A. (1994). On the temperature dependence of soil respiration. *Functional Ecology*, *8*(3), 315. https://doi.org/10.2307/2389824

Lorenz, K., & Lal, R. (2005). The depth distribution of soil organic carbon in relation to land use and management and the potential of carbon sequestration in subsoil horizons.

In *Advances in agronomy* (pp. 35–66). Elsevier. https://doi.org/10.1016/S0065-2113(05)88002-2

Lugato, E., Paustian, K., Panagos, P., Jones, A., & Borrelli, P. (2016). Quantifying the erosion effect on current carbon budget of european agricultural soils at high spatial resolution. *Global Change Biology*, *22*(5), 1976–1984. https://doi.org/10.1111/gcb.13198

Maier, M., Schack-Kirchner, H., Hildebrand, E., & Schindler, D. (2011). Soil CO2 efflux vs. soil respiration: Implications for flux models. *Agricultural and Forest Meteorology*, *151*(12), 1723–1730. https://doi.org/10.1016/j.agrformet.2011.07.006

Martin, M. P., Wattenbach, M., Smith, P., Meersmans, J., Jolivet, C., Boulonne, L., & Arrouays, D. (2011). Spatial distribution of soil organic carbon stocks in france. *Biogeosciences*, *8*(5), 1053–1065. https://doi.org/10.5194/bg-8-1053-2011

Meersmans, J., De Ridder, F., Canters, F., De Baets, S., & Van Molle, M. (2008). A multiple regression approach to assess the spatial distribution of soil organic carbon (SOC) at the regional scale (flanders, belgium). *Geoderma*, *143*(1), 1–13. https://doi.org/10.1016/j.geoderma.2007.08.025

Meersmans, J., Van WESEMAEL, B., Goidts, E., Van MOLLE, M., De BAETS, S., & De RIDDER, F. (2011). Spatial analysis of soil organic carbon evolution in belgian croplands and grasslands, 1960-2006: SPATIAL ANALYSIS OF SOIL ORGANIC CARBON EVOLUTION. *Global Change Biology*, *17*(1), 466–479. https://doi.org/10.1111/j.1365-2486.2010.02183.x

Meersmans, J., Van Wesemael, B., & Van Molle, M. (2009). Determining soil organic carbon for agricultural soils: A comparison between the walkley & black and the dry combustion methods (north belgium). *Soil Use and Management*, *25*(4), 346–353. https://doi.org/10.1111/j.1475-2743.2009.00242.x

Meyer, N., Meyer, H., Welp, G., & Amelung, W. (2018). Soil respiration and its temperature sensitivity (q10): Rapid acquisition using mid-infrared spectroscopy. *Geoderma*, *323*, 31–40. https://doi.org/10.1016/j.geoderma.2018.02.031

Oades, J. M. (1984). Soil organic matter and structural stability: Mechanisms and implications for management.

Poissant, L., Beauvais, C., Lafrance, P., & Deblois, C. (2008). Pesticides in fluvial wetlands catchments under intensive agricultural activities. *Science of The Total Environment*, *404*(1), 182–195. https://doi.org/10.1016/j.scitotenv.2008.05.030

Polyakov, V., & Lal, R. (2004). Modeling soil organic matter dynamics as affected by soil water erosion. *Environment International*, *30*(4), 547–556. https://doi.org/10.1016/j.envint.2003.10.011

Reichstein, M., Bednorz, F., Broll, G., & Kätterer, T. (2000). Temperature dependence of carbon mineralisation: Conclusions from a long-term incubation of subalpine soil samples. *Soil Biology and Biochemistry*, *32*(7), 947–958. https://doi.org/10.1016/S0038-0717(00)00002-X

Ruamps, L. S., Nunan, N., Pouteau, V., Leloup, J., Raynaud, X., Roy, V., & Chenu, C. (2013). Regulation of soil organic c mineralisation at the pore scale. *FEMS Microbiology Ecology*, *86*(1), 26–35. https://doi.org/10.1111/1574-6941.12078

Sato, J. H., Figueiredo, C. C. d., Marchão, R. L., Madari, B. E., Benedito, L. E. C., Busato, J. G., & Souza, D. M. d. (2014). Methods of soil organic carbon determination in brazilian savannah soils. *Scientia Agricola*, *71*(4), 302–308. https://doi.org/10.1590/0103-9016-2013-0306

Schmidt, M. W. I., Torn, M. S., Abiven, S., Dittmar, T., Guggenberger, G., Janssens, I. A., Kleber, M., Kögel-Knabner, I., Lehmann, J., Manning, D. A. C., Nannipieri, P., Rasse,

D. P., Weiner, S., & Trumbore, S. E. (2011). Persistence of soil organic matter as an ecosystem property. *Nature*, *478*(7367), 49–56. https://doi.org/10.1038/nature10386

Sierra, C. A., Müller, M., Metzler, H., Manzoni, S., & Trumbore, S. E. (2017). The muddle of ages, turnover, transit, and residence times in the carbon cycle. *Global Change Biology*, *23*(5), 1763–1773. https://doi.org/10.1111/gcb.13556

Six, J., Bossuyt, H., Degryze, S., & Denef, K. (2004). A history of research on the link between (micro)aggregates, soil biota, and soil organic matter dynamics. *Soil and Tillage Research*, *79*(1), 7–31. https://doi.org/10.1016/j.still.2004.03.008

Six, J., Conant, R. T., Paul, E. A., & Paustian, K. (2002). Stabilization mechanisms of soil organic matter: Implications for c-saturation of soils.

Six, J., Elliott, E., Paustian, K., & Doran, J. W. (1998). Aggregation and soil organic matter accumulation in cultivated and native grassland soils. *Soil Science Society of America Journal*, *62*(5), 1367–1377. https://doi.org/10.2136/sssaj1998.03615995006200050032x

Six, J., Paustian, K., Elliott, E. T., & Combrink, C. (2000). Soil structure and organic matter i. distribution of aggregate-size classes and aggregate-associated carbon. *Soil Science Society of America Journal*, *64*(2), 681–689. https://doi.org/10.2136/sssaj2000.642681x

Smith, P., Soussana, J.-F., Angers, D., Schipper, L., Chenu, C., Rasse, D. P., Batjes, N. H., Egmond, F., McNeill, S., Kuhnert, M., Arias-Navarro, C., Olesen, J. E., Chirinda, N., Fornara, D., Wollenberg, E., Álvaro-Fuentes, J., Sanz-Cobena, A., & Klumpp, K. (2020). How to measure, report and verify soil carbon change to realize the potential of soil carbon sequestration for atmospheric greenhouse gas removal. *Global Change Biology*, *26*(1), 219–241. https://doi.org/10.1111/gcb.14815

Stallard, R. F. (1998). Terrestrial sedimentation and the carbon cycle: Coupling weathering and erosion to carbon burial. *Global Biogeochemical Cycles*, *12*(2), 231–257. https://doi.org/10.1029/98GB00741

Stockmann, U., Adams, M. A., Crawford, J. W., Field, D. J., Henakaarchchi, N., Jenkins, M., Minasny, B., McBratney, A. B., Courcelles, V. d. R. d., Singh, K., Wheeler, I., Abbott, L., Angers, D. A., Baldock, J., Bird, M., Brookes, P. C., Chenu, C., Jastrow, J. D., Lal, R., … Zimmermann, M. (2013). The knowns, known unknowns and unknowns of sequestration of soil organic carbon. *Agriculture, Ecosystems & Environment*, *164*, 80–99. https://doi.org/10.1016/j.agee.2012.10.001

Tan, Z., Lal, R., Owens, L., & Izaurralde, R. (2007). Distribution of light and heavy fractions of soil organic carbon as related to land use and tillage practice. *Soil and Tillage Research*, *92*(1), 53–59. https://doi.org/10.1016/j.still.2006.01.003

Trumbore, S., & Barbosa de Camargo, P. (2009). Soil carbon dynamics. In M. Keller, M. Bustamante, J. Gash, & P. Silva Dias (Eds.), *Geophysical monograph series* (pp. 451–462). American Geophysical Union. https://doi.org/10.1029/2008GM000741

Van Hemelryck, H., Govers, G., Van Oost, K., & Merckx, R. (2011). Evaluating the impact of soil redistribution on the in situ mineralization of soil organic carbon. *Earth Surface Processes and Landforms*, *36*(4), 427–438. https://doi.org/10.1002/esp.2055

Van Oost, K., Govers, G., De Alba, S., & Quine, T. A. (2006). Tillage erosion: A review of controlling factors and implications for soil quality. *Progress in Physical Geography: Earth and Environment*, *30*(4), 443–466. https://doi.org/10.1191/0309133306pp487ra

Van Oost, K., Govers, G., Quine, T. A., Heckrath, G., Olesen, J. E., De Gryze, S., & Merckx, R. (2005). Landscape-scale modeling of carbon cycling under the impact of soil redistribution: The role of tillage erosion: TILLAGE EROSION AND CARBON DYNAMICS. *Global Biogeochemical Cycles*, *19*(4), n/a–n/a. https://doi.org/10.1029/2005GB002471

van Wesemael, B., Lettens, S., Roelandt, C., & Orshoven, J. V. (1960). Changes in soil carbon stocks from 1960 to 2000 in the main belgian cropland areas.

von Lützow, M., Kögel-Knabner, I., Ekschmitt, K., Flessa, H., Guggenberger, G., Matzner, E., & Marschner, B. (2007). SOM fractionation methods: Relevance to functional pools and to stabilization mechanisms. *Soil Biology and Biochemistry*, *39*(9), 2183–2207. https://doi.org/10.1016/j.soilbio.2007.03.007

Wang, Y., Zhang, J., Zhang, Z., & Jia, L. (2016). Impact of tillage erosion on water erosion in a hilly landscape. *Science of The Total Environment*, *551-552*, 522–532. https://doi.org/10.1016/j.scitotenv.2016.02.045

Zhao, L., Sun, Y., Zhang, X., Yang, X., & Drury, C. (2006). Soil organic carbon in clay and silt sized particles in chinese mollisols: Relationship to the predicted capacity. *Geoderma*, *132*(3), 315–323. https://doi.org/10.1016/j.geoderma.2005.04.026

Appendices

A SOC content depth distribution at each study plot (values listed in table 2)

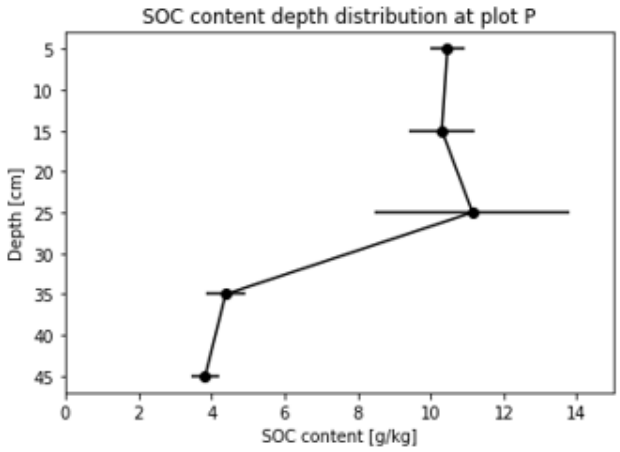

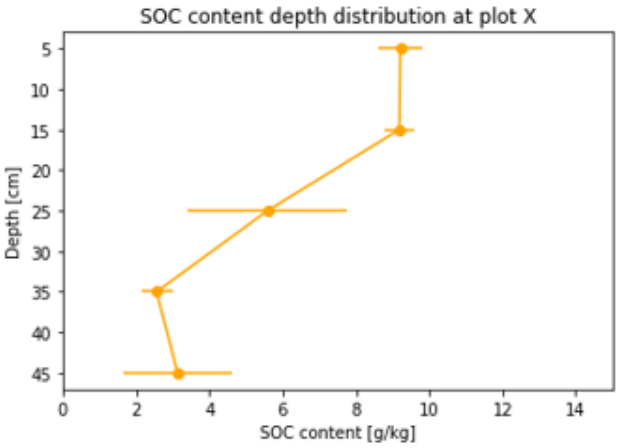

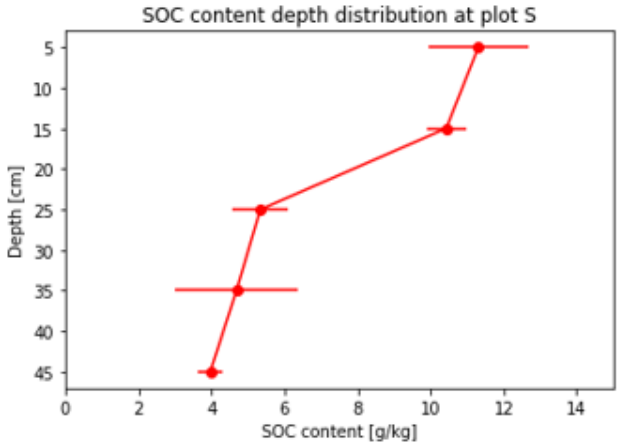

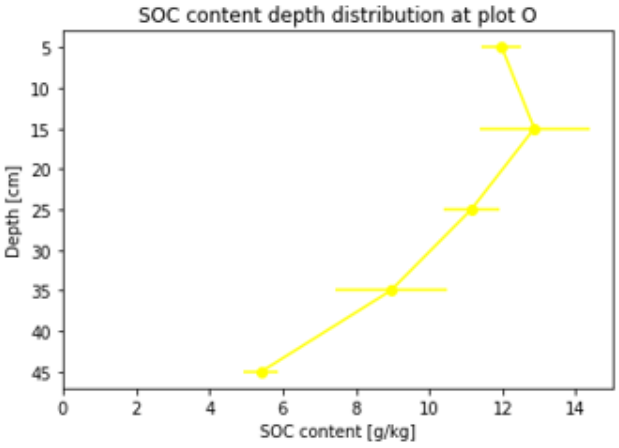

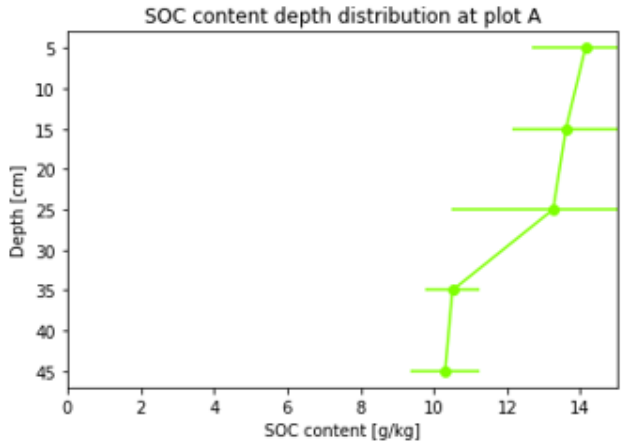

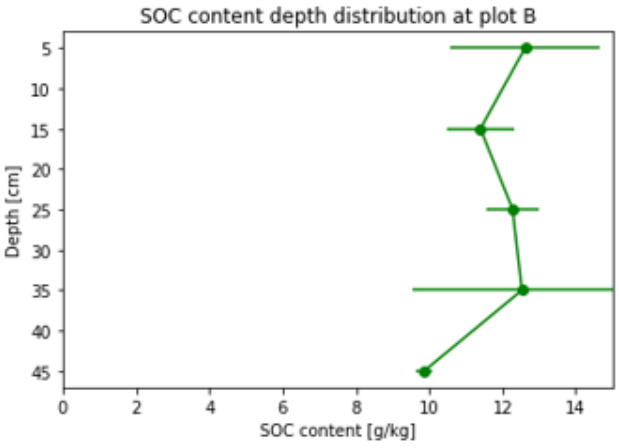

B Soil bulk density depth evolution at each study plot (values listed in table 3)

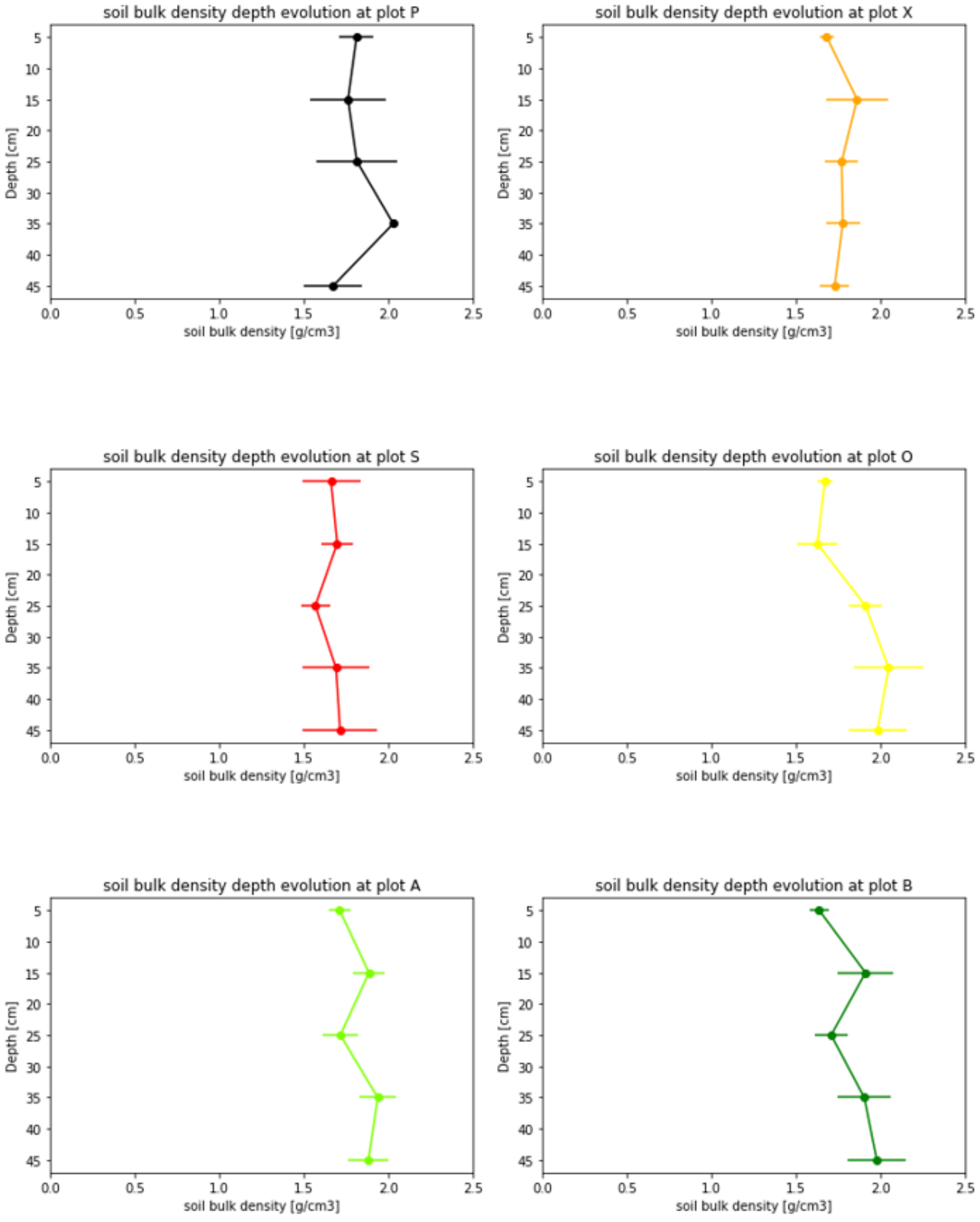

C Tillage erosion (left) and water erosion (right) rates on the study field calculated by P. Baert, with the use of the Watem/Sedem model on a 20x20m resolution.

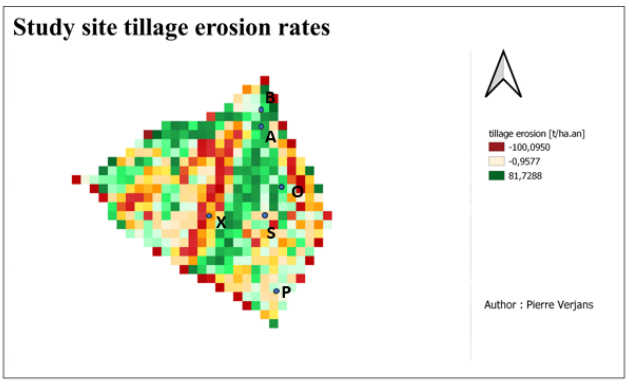

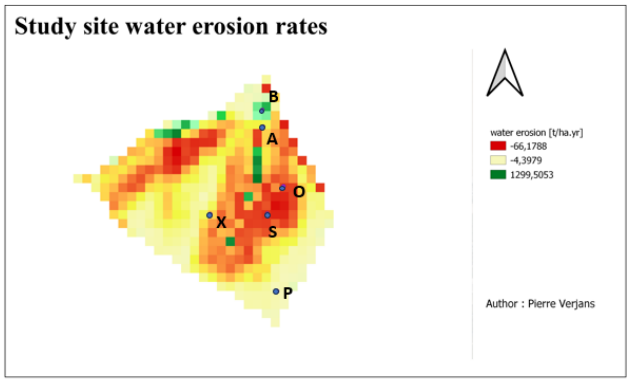

D Colour differences in the study field evidencing the three different cultivated varieties of wheat.

E soil core showing the 0-80cm pedological profiles of plot P (a), and X (b)

(a)

(b)

F soil core showing the 0-80cm pedological profiles of plot S (c), and O (d)

(c)

(d)

G soil core showing the 0-80cm pedological profiles of plot A (e), and B (f)

(e)

(f)

H Measured daily mean mineralisation rates at each plot associated with their standard deviation.

	Soil C mineralisation rate *10E-3 [mgC/gCsoil.hr]					
Day	P	X	S	O	A	B
0	10.24 ± 2.26	20.80 ± 4.97	17.28 ± 2.48	9.60 ± 4.08	9.65 ± 2.57	16.73 ± 3.57
11	10.75 ± 1.95	27.78 ± 1.63	19.21 ± 3.05	15.69 ± 2.88	12.78 ± 2.77	13.59 ± 2.76
25	12.28 ± 2.70	18.44 ± 5.30	15.46 ± 1.07	10.97 ± 2.15	8.71 ± 1.65	11.69 ± 2.97
34	16.77 ± 2.48	27.56 ± 3.95	23.28 ± 2.65	16.14 ± 3.57	13.41 ± 1.61	12.53 ± 1.32
46	14.93 ± 8.50	38.67 ± 5.04	34.61 ± 7.66	20.95 ± 8.20	15.63 ± 3.02	17.37 ± 2.28
52	21.59 ± 3.01	20.25 ± 5.34	19.04 ± 2.65	17.52 ± 4.89	11.59 ± 3.14	11.90 ± 1.70
61	17.10 ± 2.99	28.63 ± 6.59	20.66 ± 1.53	16.33 ± 4.33	12.39 ± 1.71	14.53 ± 1.46
77	19.58 ± 2.37	23.22 ± 4.15	19.70 ± 2.51	15.59 ± 2.19	13.51 ± 1.74	16.26 ± 1.84
87	32.27 ± 0.82	37.31 ± 4.18	33.94 ± 4.48	20.18 ± 4.88	13.91 ± 1.52	12.30 ± 1.52
95	18.46 ± 0.85	22.58 ± 2.78	20.35 ± 1.67	17.29 ± 3.68	12.22 ± 1.54	12.95 ± 1.09
104	17.57 ± 3.55	21.61 ± 1.81	18.75 ± 1.73	15.30 ± 1.83	12.78 ± 1.48	15.08 ± 1.87

I Aerian vue of the study field in 1971 (WalOnMap)